TECHNICAL REPORT 2071
March 2014

Counter Tunnel Project Final Report

Jacoby Larson
David Hooper
Jim Edwards
Tracy Heath Pastore
Ryan Halterman
Brian Okorn
SSC Pacific

Brian Skibba
AFRL

SSC Pacific
San Diego, CA 92152-5001

SSC Pacific
San Diego, California 92152-5001

K. J. Rothenhaus, CAPT, USN
Commanding Officer

C. A. Keeney
Executive Director

ADMINISTRATIVE INFORMATION

The work described in this report was performed by the Unmanned Systems Science & Technology Branch (Code 71710) and the Unmanned Systems Advanced Development Branch (Code 71720), Space and Naval Warfare Systems Center Pacific (SSC Pacific), San Diego, CA, and the Air Force Robotics Laboratory Airbase Technologies Division (AFRL/RXQ), Tyndall Air Force Base, Panama City, FL.

Released by
T. Pastore, Head
Unmanned Systems Science
& Technology Branch

Under authority of
A. D. Ramirez. Head
Advanced Systems & Applied
Sciences Division

ACKNOWLEDGMENTS

The authors gratefully acknowledge the funding and oversight of the Joint Ground Robotics Enterprise and for the time and support of the Customs and Border Patrol to provide logistics and support to test and collect data inside multiple cross-border tunnels.

SB

EXECUTIVE SUMMARY

Covert cross-border tunnels are a security vulnerability that enables people and contraband to illegally enter the United States. All of these tunnels have been utilized for the purpose of drug- and human-smuggling, but they may also be used to support terrorist attacks against the United States. Past robotic tunnel exploration efforts have had limited success in aiding law enforcement to explore and map suspect cross-border tunnels. These efforts have used adapted explosive ordnance disposal (EOD) or pipe-inspection robotic systems that are not ideally suited to the cross-border tunnel environment.

This *Counter Tunnel* project developed a prototype robotic system for counter-tunnel operations to provide law enforcement agencies and the warfighter with a capability for assessing tunnel-like environments without sending in personnel into the confined space. The effort focused on technology solutions for localizing, exploring, mapping, and characterizing tunnels, identifying items of interest, and locating the point(s) of entry. It was sponsored by the Office of the Under Secretary of Defense (OUSD) Joint Ground Robotics Enterprise (JGRE) and jointly executed by Air Force Research Laboratory Airbase Technologies Division (AFRL/RXQ) Tyndall and SPAWAR Systems Center (SSC) Pacific. The *Counter Tunnel* project was a complementary development effort to the Rapid Reaction Tunnel Detection (R2TD) Joint Capability Technology Demonstration (JCTD), managed by U.S. Northern Command (USNORTHCOM).

The prototype counter-tunnel system developed under this effort is composed of a robotic mobility platform, perception sensor payload, onboard autonomy capability, command and control operator unit, and deployment apparatus. The overall design was driven by the requirement to deploy the system into a tunnel through a 20-centimeter-diameter borehole. This requirement posed many design and packaging challenges for the perception payload and mobility platform in order to fit through the narrow borehole opening and still be able to perform the mission in a GPS-denied environment.

The *Counter Tunnel* project presented a unique prototype UGV mobility platform capable of insertion and retrieval through the 20-centimeter-diameter borehole, climbing 30-centimeter vertical steps, and crossing 30-centimeter gaps. This project also demonstrated a perception system capable of performing obstacle detection, 3D mapping, and GPS-denied localization with an error of 0.1% after traveling autonomously for 900 meters through a tunnel-like environment. This project has increased the technology readiness level of various components of the counter-tunnel systems (platforms, sensors, communications, and payloads) and has advanced the work in GPS-denied navigation, 3D perception, and mapping. The prototype evaluations and expertise gained from this work will be key to providing robust and deployable systems to explore tunnels, caves, mines, and similar environments.

CONTENTS

1. INTRODUCTION **1**

1.1 PURPOSE 1

1.2 BACKGROUND 1

1.3 OBJECTIVES AND SCOPE 2

1.4 SYSTEM REQUIREMENTS 2

2. BOREHOLE DEPLOYMENT/RETRIEVAL APPARATUS **3**

2.1 BOREHOLE DEPLOYMENT/RETRIEVAL APPARATUS TESTING 5

3. ROBOTIC PLATFORMS **6**

3.1 PROTOTYPE *COUNTER TUNNEL EXPLOITATION ROBOT* (*CTER*) PLATFORM 6

3.1.1 *CTER* Testing 6

3.2 ALTERNATIVE PLATFORMS 10

3.2.1 iRobot® *PackBot®* 10

3.2.2 RoboteX® *AVATAR® II* 11

3.2.3 Unmanned Aerial Vehicles 11

4. COMMUNICATIONS **13**

4.1 COMMUNICATIONS REQUIREMENTS 13

4.2 RADIO SELECTION TESTING 13

4.3 RADIO SELECTION 13

4.4 RADIO TESTING 13

4.5 RADIO DOWNSELECT 15

5. PERCEPTION **16**

5.1 PERCEPTION SENSOR 16

6. LOCALIZATION AND MAPPING **19**

6.1 BOREHOLE APPARATUS LOCALIZATION 19

6.1.1 Kearfott Accuracy Test Results 20

6.1.2 Borehole Insertion Testing 20

6.2 FIDUCIAL LOCALIZATION 21

6.2.1 Fiducial Pattern 21

6.2.2 Localization Algorithm 23

6.2.3 Fiducial Localization Testing 26

6.3 VEHICLE LOCALIZATION 26

6.3.1 *MultiSense-SL* Localization 26

6.3.2 Alternative 2D Mapping Localization 26

6.4 SLIDE IMAGES 30

6.5 STRUCTURE FROM MOTION 33

7. AUTONOMY **35**

7.1 SOFTWARE: *AUTONOMOUS CAPABILITY SUITE (ACS)* 35
8. *MULTI-ROBOT OPERATOR CONTROL UNIT (MOCU)* **36**
9. SYSTEM TESTING AND DEMONSTRATION **37**
9.1 JOINT AFRL/SSC PACIFIC DEMONSTRATION 38
9.2 DEMONSTRATION AND TEST WITH U.S. CUSTOMS AND BORDER PROTECTION 38
9.3 DATA COLLECTION OF CROSS-BORDER TUNNEL 41
10. FUTURE WORK **47**
11. CONCLUSION **49**
REFERENCES **49**

FIGURES

1. Robot Delivery Capsule (RDC) model with labeled parts. 3
2. Robot Delivery Capsule (RDC). 4
3. Capsule Support Trailer. 4
4. *CTER* platform maneuvering around obstacles. 7
5. *CTER* platform driving into a 23-centimeter storm drain. 7
6. *CTER* platform in *Tank* mode in a test tunnel. 8
7. *PackBot®* with mounted NREC *MultiSense-SL*. 10
8. *AVATAR® II* mounted with sensors and radios. 11
9. Antenna testing at Twentynine Palms test mine. 14
10. Plot of amplitude vs. frequency for wireless communication tests. 14
11. (a) Silvus radio, (b) Trellisware radio, and (c) Cobham radio. 14
12. (a) Entrance, (b) tunnel, and (c) shoring of the Eagle Mine in Julian, CA. 15
13. NREC *MultiSense-SL* perception sensor. 16
14. Point cloud of lab buildings. 17
15. Point cloud of lab space. 18
16. System localization error. 19
17. Deployment of the *CTER* platform. 22
18. 5 x 8 cylindrical fiducial pattern. 22
19. 5 x 16 cylindrical fiducial pattern. 22
20. 10 x 10 planar fiducial pattern. 23
21. Contour detection on cylindrical fiducial pattern in mock tunnel. 24
22. Fiducial matching to a cylindrical pattern. 25
23. Fiducial matching to a tilted cylindrical pattern. 25
24. *MultiSense-SL* mounted on a *PackBot®* 27
25. Registered point cloud of a storm drain and manhole cover. 27
26. *CTER* platform with mounted Hokuyo lidar sensor (lower left). 28
27. Lab facilities map created by *Hector Mapping* with errors from loop closure. 29
28. Localization error from *Hector Mapping*. 30
29. Scan segmentation for slide image generation. 31
30. Slide image tunnel segment. 31
31. Gaussian blurred slide image histogram. 32
32. Accuracy of uninitialized ICP and slide image pair-wise registration. 32
33. Cross-border Marconi tunnel steep downward steps. 33
34. Cross-border Marconi tunnel 3D reconstruction. 34
35. Screenshot of *MOCU* controlling a *PackBot®* in lab space. 36
36. Various test tunnels. 37
37. The *PackBot®* autonomously traversing a storm drain. 39
38. Point cloud of storm drain. 39
39. *AVATAR® II* robot equipped with sensors and radios. 40
40. *CTER* platform about to enter a 45-centimeter storm drain. 40
41. *CTER* platform beginning to traverse sandy terrain in a storm drain. 41
42. Rail and cart system in a cross-border tunnel discovered by the Border Patrol. 42
43. *PackBot®* with mounted with autonomy hardware. 43
44. Point cloud of tunnel, captured from the *MultiSense-SL* sensor. 43
45. Point cloud of steps leading down into the tunnel. 44
46. Point cloud of tunnel and warehouse merged with aerial lidar point cloud. 44

47. Overhead view of point cloud of tunnel with drilling points. 45
48. *Google Earth*™ image with overlayed estimated drilling points. 46
49. *Google Earth*™ image with overlayed estimated and real drilling points. 46

TABLES

1. *CTER* drive times and distances in various drive modes. 8
2. Kearfott INU specifications versus requirements. 20
3. Kearfott accuracy test data (azimuth, pitch, and roll measurements are in degrees). 21

1. INTRODUCTION

1.1 PURPOSE

The purpose of the *Counter Tunnel* project is to develop a prototype robotic system that provides the warfighter and law enforcement with a safe and effective solution for exploration, localization, mapping, and characterization of a tunnel-like environment, identifying items of interest, and locating the point(s) of entry.

1.2 BACKGROUND

Illegal international border crossings into the United States through man-made tunnels and utility culverts have become more prevalent. In particular, the border between Mexico and the southwestern United States is a target for drug-smugglers bringing illegal drugs into the United States. Many technological and legal problems exist in detecting, securing, and decommissioning these tunnels. Often, these access tunnels are tens to hundreds of meters long, can have significant elevation gradients, and may contain water and/or various types of debris.

There are several categories of tunnels being built to gain entry into the U.S., widely ranging in depth and dimensions. They can be elaborate (sophisticated, symmetric, professionally engineered), or hastily built (hand dug, shallow, unreinforced). Some tunnels are designed to connect into city storm drain systems, allowing circumvention of the border, such as in Nogales, Arizona. A few tunnels have been documented to be over a mile long. The extreme variances in conditions that exist within the tunnels, and the fact that many are used sporadically, make identifying their existence and locating access points a difficult task.

The Department of Defense (DoD) has three combatant commands with interests in tunnels, both domestically and abroad. U.S. Strategic Command (USSTRATCOM) is concerned with combating weapons of mass destruction (WMD). U.S. Central Command's (USCENTCOM) area of responsibility (AOR) includes current areas susceptible to tunneling in Iraq, Afghanistan, Egypt, Israel, and potentially other countries. U.S. Northern Command's (USNORTHCOM) mission is to defend, protect, and secure the United States and its interests, including support of counter-drug operations and managing the consequences of terrorist events employing WMDs. USNORTHCOM's AOR includes the U.S., Mexico, and Canada, and providing assistance to lead law enforcement agencies when tasked by the DoD. This project developed a capability to explore tunnels and identify the entrances to illegal tunnels crossing over U.S. borders, and to exploit voids within theaters of operation overseas.

Previous work performed with robots working in tunnels and mines for teleoperation and mapping and has been leveraged by this project. Some of the earlier work, documented by Laird [1], laid out some of the basic vehicle teleoperation issues for tunnel exploration and reconnaissance. Mapping tunnels and mines tends to be difficult because of the relatively nondescript nature of the walls, which is why many of these tunnel/mine-mapping systems integrate lidars into their localization systems [2]. Carnegie Mellon University (CMU) used a nodding lidar and registered the data using Simulataneous Localization and Mapping (SLAM) [3]. Other mine-mapping systems have used stop/start scanning with two-dimensional (2D) lidars [4] which involves obstacle avoidance while the vehicle is moving, then stopping to allow the robot to generate a stable three-dimensional (3D) scan of the environment. This 3D data was then used with Markov Random Fields, an A* search, and C-space maps to generate 3D maps and plan future motion. Nüchter et al. [5] discussed a 3D SLAM algorithm designed to handle the six degrees of freedom (6DoF)

inherent in a subterranean environment, using a reduced point cloud and a fast iterative closest point (ICP) variant to locally and globally register the point clouds.

This counter-tunnel effort was funded by the Joint Ground Robotics Enterprise (JGRE) from fiscal year 2010 through 2013, run jointly by SPAWAR Systems Center (SSC) Pacific and Air Force Robotics Laboratory Airbase Technologies Division (AFRL/RXQ) Tyndall, and was a complementary development effort addressing objective requirements to the Rapid Reaction Tunnel Detection (R2TD) Joint Capability Technology Demonstration (JCTD), managed by U.S. Northern Command (USNORTHCOM). This project addresses the objective tunnel exploration requirements defined for the R2TD JCTD.

1.3 OBJECTIVES AND SCOPE

The project objective is to develop and demonstrate technologies that enable insertion of a robotic system through a small borehole into a suspect tunnel cavity to conduct precision mapping and characterization operations in austere tunnel environments (hand-dug border tunnels, caves, etc.).

The scope of the effort has been divided into three major technology thrusts:

1. Development of an Unmanned Ground Vehicle (UGV) mobility platform capable of insertion through a maximum 20-centimeter-diameter borehole.
2. Development of a borehole deployment capsule to support insertion and retrieval of the UGV system and provide a communications relay node at the tunnel insertion point.
3. Development of a perception system small enough to fit inside the borehole deployment capsule and provide localization, obstacle detection, and 3D mapping.

1.4 SYSTEM REQUIREMENTS

- Deploy and retrieve a UGV through a 20-centimeter borehole into tunnels 3 to 30 meters in depth
- Transit up to 800-meter round trip
- Traverse two horizontal 45-degree turns
- Climb a 30-centimeter vertical discontinuity (i.e., a step)
- Traverse a 30-centimeter gap or crevice
- Operate over varied and rough terrain including mud, loose gravel, areas of limited traction, and up to 20 centimeters of standing water
- Autonomously explore, localize, and map the tunnel
- Localize the entry within 1 meter of accuracy
- Generate a 3D model of the tunnel environment for characterization, measurement, and analysis

2. BOREHOLE DEPLOYMENT/RETRIEVAL APPARATUS

The Borehole Deployment/Retrieval Apparatus was developed by the Air Force Research Laboratory Airbase Technologies Division (AFRL/RXQ) Tyndall Robotics Team, its main purpose being to deliver the intended UGV platform, the Counter Tunnel Exploitation Robot (*CTER*), through a 20-centimeter borehole to depths of up to 30 meters. The apparatus is composed of two parts: the Robot Delivery Capsule (RDC) and the Capsule Support Trailer.

The Robot Delivery Capsule, in Figures 1 and 2, is a unique system that safely stores the *CTER* during deployment and retrieval through a 20-centimeter borehole. The Kearfott *KI-4901* inertial measurement unit (IMU) aboard the RDC provides a highly accurate initial position and orientation for the mapping sensor. An internal winch is used to lower and raise the *CTER* into and out of the RDC. A clasping device securely holds the robot in place during this operation, keeping the robot in a fixed orientation to the RDC for transferring the initial position to the robot. A camera and light at the end of the RDC helps to aid the operator execute this process.

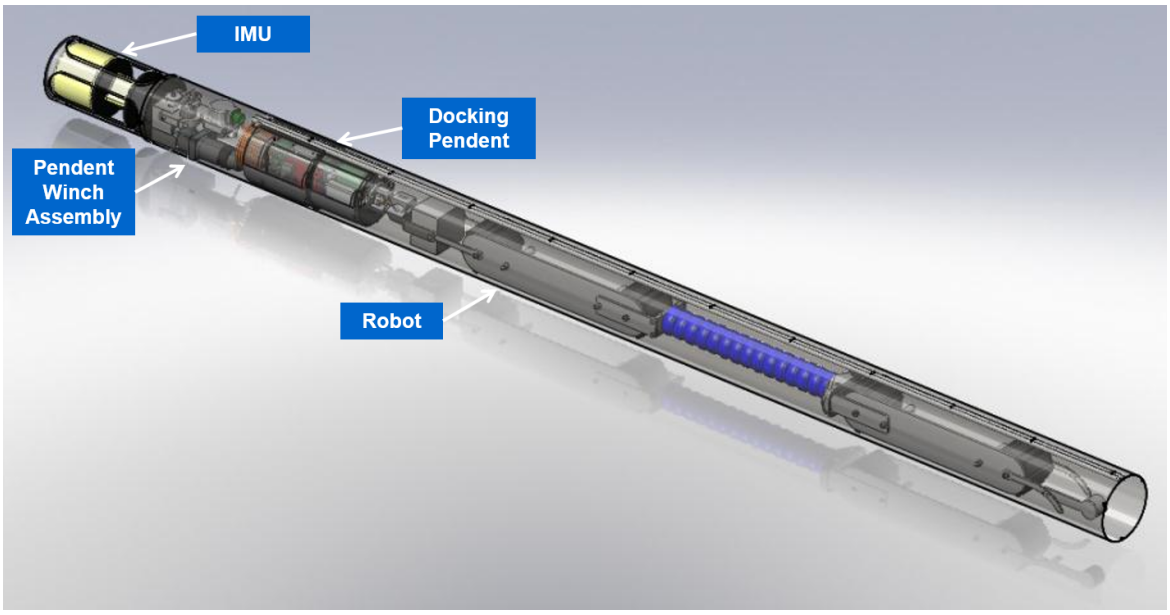

Figure 1. Robot Delivery Capsule (RDC) model with labeled parts.

The Capsule Support Trailer, Figure 3, also includes a winch to raise and lower the RDC to the appropriate borehole depths. The winch cable is run over a pulley on top of a vertical A-frame mounted on the rear of the trailer. A control box for remote control of the RDC as well as the trailer-mounted winch is located near the tongue of the trailer. Supporting stands are also provided on the trailer for stowage of the RDC during transport of the system.

The trailer instrumentation monitors weight and position feedback for RDC deployment. A generator mounted on the trailer provides power for the RDC, the trailer-mounted winch, the system control box, and any command and control computers needed for the system. The trailer also has hand-cranked lifts mounted on the corners to level the trailer prior to deployment of the RDC.

Figure 2. Robot Delivery Capsule (RDC).

Figure 3. Capsule Support Trailer.

2.1 BOREHOLE DEPLOYMENT/RETRIEVAL APPARATUS TESTING

Engineers conducted suitability and functionality testing on the Borehole Deployment/Retrieval Apparatus, including the Capsule Support Trailer and the RDC. They tested the Deployment Trailer's Sound Ocean Systems, Inc. *ECO Winch* for suitability for RDC deployment. The winch measurement was not used for cable length since it only had a 30-centimeter resolution. The BEI Sensors *H25* incremental optical encoder was used to verify the cable length readings from the IMU on the depth of the tunnel and to provide feedback to the RDC scripts for smooth deployment of the robot. The encoder was accurate to within 0.25% of total distance traveled. The cable management and A-frame arms were sufficient for deployment of the RDC. Gigabit multi-mode fiber-optic communication and 48 VDC power were passed to the RDC through the winch cable via a slip ring provided on the winch. This South Bay Cable *SB-47575* has a working load strength of 200 pounds and a breaking strength of 1000 pounds. A Strainsert *Q21880* clevis bolt served as the axle for the pulley wheel over which the winch cable was passed, and used to measure the weight on the cable and as an indicator if the RDC was stuck in the borehole. Drive current to the winch motor was also monitored for this purpose with AcuAMP *ACT050* current sensors. The control box monitoring all of the information, as well as the source of the 48 VDC and fiber-optic cable to the RDC, was designed and built by AFRL. This control box was powered by 115 VAC and used Gigabit Ethernet for communications.

The Robot Delivery Capsule was designed to be suitable for deployment/retrieval of the *CTER*. The RDC holds the 50-pound *CTER* in a fixed position with a safety factor of six (tested to hold six times its weight). The Kearfott IMU provided position accuracy within 0.1% of distance traveled from its initial position. The measured roll of the IMU was within 0.07 degrees root-mean-square (RMS), pitch was within 0.06 degrees RMS, and yaw was within 0.03 degrees RMS of actual movement. The RDC overall length was approximately 4 meters: 1.5 meters for the electronics and internal robot attachment and 2.5 meters for *CTER* storage space. The top portion of the RDC included the IMU, an embedded computer, motor controllers, power conditioning, as well as the winch to insert and deploy the *CTER* from the RDC. This winch connected to a pendant with a unique grapple mechanism for robot attachment. Inside this pendant was a fiber-optic module for connection to the *CTER*, a camera and lighting for operator awareness, and power conditioning. A unique pattern was printed and attached on the end of the RDC, used by the mapping sensor on the UGV to determine its starting point relative to the RDC for localization to the world-coordinate system (see Section 6.2). A custom coil cable made by Woven Electronics interconnected the top section of the RDC to the pendant. This cable prevents snags on the internal winch cable as well as protects the fiber-optic and copper wires in the cable.

3. ROBOTIC PLATFORMS

3.1 PROTOTYPE *COUNTER TUNNEL EXPLOITATION ROBOT* (*CTER*) PLATFORM

The *Counter Tunnel Exploitation Robot* (*CTER*), built by Raytheon Sarcos Integrated Defense Systems (IDS), is a high degree of freedom (DOF) UGV designed to address the counter-tunnel mission as shown in Figures 4, 5, and 6. Two of these platforms were delivered: one to AFRL Robotics at Tyndall AFB, FL, and one to SSC Pacific Unmanned Systems Branch, San Diego, CA.

The *CTER* has a camera mounted on arms at the rear of the aft track, which can rotate 180 degrees to the left and right for 360-degree viewing. Arms on the front track allow for payload attachment. The *CTER* is 17 centimeters wide x 172 centimeters long x 17 centimeters tall (no payload). The robot features a fiber-optic communication tether that provides a link for commands, status, video feedback, and mapping sensor data. Wireless communication has been explored for this application and a solution is described in Section 4. The *CTER* has an on-board real-time controller for joint control, drive-motor control, and camera-image compression. The unique joints and motors arrangement between the tracks of the *CTER* allow for step climbing, roll prevention, and side-by-side track operation. The robot is also designed to be submerged in up to 20 centimeters of water (although no submersion tests were performed during this project).

Multiple drive modes are available to the robot operator including: *Find Zeroes*, *Uncommanded*, *Zero Torque*, *Step Climb*, *Anti-Roll*, *Bend*, *Follow-the-Leader*, *Cobra*, and *Tank*. The *Find Zeroes* mode is the initialization procedure that the robot needs to run every time it is powered on. The *Uncommanded* and *Zero Torque* modes disable all robot motion, and allow an operator to manipulate it manually with no motor driving. *Step Climb* driving mode will successfully climb 30-centimeter steps. *Anti-Roll* mode is a driving mode that offsets the tracks and actively corrects for roll. If a condition occurs where the mode cannot prevent a roll, the robot will go into the *Uncommanded* mode. *Bend* mode is a driving mode that allows the operator to offset the tracks at varying angles in order to provide stability. Preset angles of 15, 30, and 45 degrees are available. When rotating in this mode, the tracks turn toward each other in a C-shape. *Follow-the-Leader* is another driving mode in which the rear track attempts to follow the path of the front track exactly (Figure 4). *Cobra* mode raises the aft track in order to give the camera a better vantage point. In *Tank* mode (Figure 6), the robot will position the tracks in parallel with each other and operate as a skid-steer vehicle.

3.1.1 *CTER* Testing

The *CTER* began operation in February 2013 through June 2013. Engineers evaluated the multiple driving modes, vehicle mobility, vehicle run-time, and ease in deploying and retrieving the vehicle from the RDC.

3.1.1.1 Test: Driving Modes and Run Times.

The *CTER* standard driving operation is as follows:

1. Insert fully charged batteries into front and rear track compartments (front battery is for payloads, rear battery is for driving motors).
2. Plug in the fiber-optic communication cable from the Operator Control Unit (OCU) to the connector in the rear track compartment.
3. Install the watertight covers over both battery compartments.
4. Turn on the power to both front and rear compartments and install switch-hole plug.

Figure 4. *CTER* platform maneuvering around obstacles in a narrow tunnel in *Follow-the-Leader* mode.

Figure 5. *CTER* platform driving into a 23-centimeter storm drain.

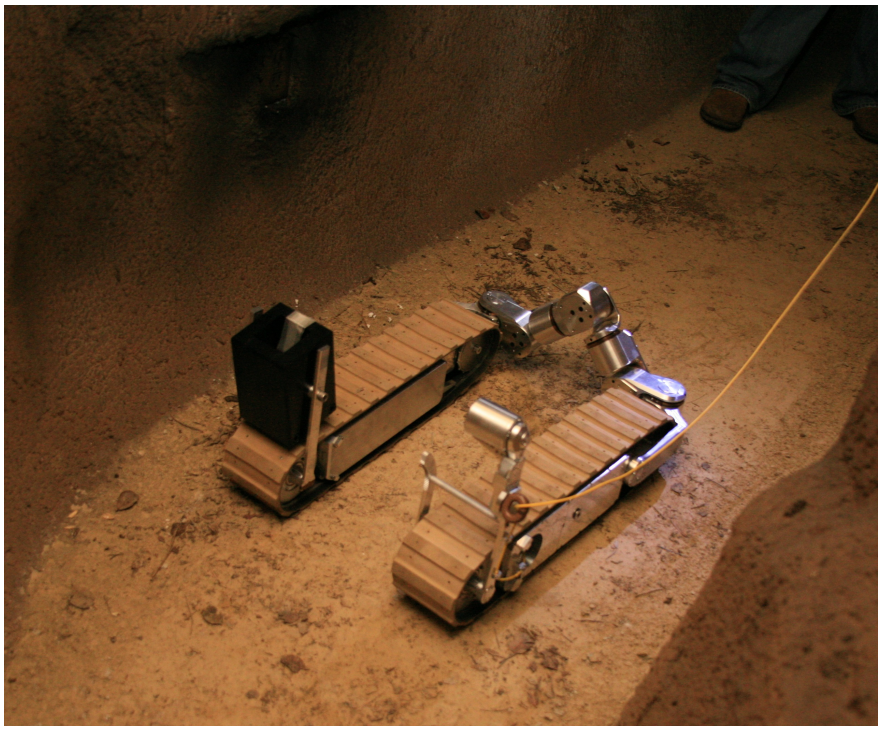

Figure 6. *CTER* platform in *Tank* mode in a test tunnel. This mode was used to turn the *CTER* around in narrow passages such as seen here.

5. Turn on the OCU and run the *Find Zeroes* mode on the robot. This mode initializes the robot for operation.
6. Select a driving mode on the OCU and operate the robot

The vehicle run time was evaluated for each driving mode in a straight run, flat gravel surface, fully charged battery, no payload installed, and until the battery was completely discharged, with results shown in Table 1.

Table 1. *CTER* drive times and distances in various drive modes.

MODE	DISTANCE	TIME
Anti-Roll	1356 m	69 min, 14 sec
Bend	1920 m	115 min, 57 sec
Follow-the-Leader	2240 m	112 min, 42 sec
Tank	2156 m	122 min, 32 sec

The *Tank* mode is the most stable of all the drive modes, however in this mode the payload is facing the rear of the robot. The *Anti-Roll* mode is currently tuned to prevent roll by the robot in the basic configuration with no payload. Adding a payload and running in this mode causes continual overcorrection by the robot, which in some cases causes the payload to hit the ground on both sides as the robot oscillates about the roll axis. With a payload installed, tests have found that *Bend* mode and *Follow-the-Leader* mode provide the most effective driving.

The *Step* mode of the robot was also evaluated, and it successfully climbed 30-centimeter steps, although the steps needed to have a front face for the tracks to drive up. The robot also demonstrated crossing a 30-centimeter gap in all driving modes.

3.1.1.2 Test: Mobility. The mobility testing of the *CTER* was to evaluate its ability to turn around in a tunnel, climb up and down 30-centimeter steps, drive in 91-centimeter culverts, turn around in 91-centimeter culverts, drive over gaps of 30 centimeters, and evaluate effectiveness of fiber-optic spools for control of the robot.

Turning the *CTER* around in a small space was very challenging. It was determined when driving in *Bend* or *Follow-the-Leader* mode that putting the robot in *Tank* mode, turning around, and returning to the previous drive mode was the easiest way to turn around.

The *CTER* could climb up and down 30-centimeter steps. However, climbing required a flat floor surface and sufficient floor-surface friction. Polished concrete provides insufficient friction for the snake to climb the stairs. Plywood, gravel, and carpet were all adequate floor surfaces to allow the *CTER* to climb steps.

Driving in 91-centimeter round culverts was successful but required a close watch on the roll angle while driving. Since the culvert had no reference points to look at while driving, the roll indicator was the only way to determine if the *CTER* was driving at the bottom of the culvert. Without the roll indicator, rollovers of the *CTER* are expected. Turning around in the culvert was accomplished using *Tank* mode.

The *CTER* can cross 30-centimeter gaps without any extra effort. Due to the track length being almost double the 30-centimeter gap size, there was no visually perceptible drop on the front of the track when crossing a 30-centimeter gap.

The *CTER* platform was designed to use fiber-optic spools for communications. Due to difficulties in obtaining properly wound fiber-optic spools before the test events, fiber spool testing was not completed. All of the tests at AFRL were accomplished via an unspooled 823-meter test fiber-optic cable.

As previously mentioned, the *CTER* is a prototype robot design, built to meet the requirements of delivery through a 20-centimeter borehole, driving 800 meters, and communicating via fiber-optics. Although this platform met these requirements, there were some observed reliability issues. Both of the delivered *CTER* platforms had to have the joints of the center section replaced as a result of cold welding between the original joints. Additionally, a track controller circuit board had to be replaced due to a failure. The power-up calibration sequence was also sometimes problematic, as it would occasionally initialize in the wrong orientation. This would then require a reboot and rerun of the calibration sequence until it was performed correctly. A couple months after initial receipt of the AFRL *CTER*, it had to be returned to the manufacturer for an upgrade. This upgrade put a real-time controller on board the *CTER* and seemed to improve the responsiveness of the controls. A shipping container designed specifically for the *CTER* was also built due to problems encountered during shipping of the *CTER* at SSC Pacific. The time required for these fixes and upgrades greatly limited the amount of time available for subsequent testing and evaluation of the *CTER* platform.

3.1.1.3 Test: Terrain Maneuvers. The *CTER* was driven over varied terrain and performed well (without the localization and mapping payload). Using the *Anti-Roll* mode, the platform was able to drive over gravel, crushed rock, and obstacles such as pieces of 2- x 4-inch lumber without tipping over. Large obstacles such as a pile of 15- to 30-centimeter rocks were found to be too difficult for the *CTER* to navigate, and climbing over these obstacles often resulted in roll-over, even in the *Anti-Roll* driving mode. In other modes such as *Bend* and *Follow-the-Leader*, the snake successfully navigated the previously mentioned

obstacles but required care to prevent tip-over. When tip-overs did occur, operators used the *CTER*'s *Roll* mode to roll the robot to the upright position. Corrugated plastic and steel also presented no traversal problems.

The *CTER* was designed to withstand submersion in up to 20 centimeters of water, although this could not be verified because water tightness of the *CTER* was only accomplished with installation of a fiber spool. As discussed earlier in Section 3.1.1.2, the fiber spools were not delivered in time for testing by AFRL.

3.2 ALTERNATIVE PLATFORMS

SSC Pacific created a plan to use alternative robotic platforms for testing and evaluation of sensors and autonomy algorithms, to continue development work while the *CTER* platform was being prototyped and upgraded. Although these alternative platforms would not fit through a 20-centimeter borehole, they could still be viable options for ISR, mapping, and characterization of tunnels if other methods of entry were available.

3.2.1 iRobot® *PackBot®*

The iRobot® *PackBot®* was the primary vehicle for sensor and autonomy development. SSC Pacific has used the *PackBot®* in various other projects and even developed a teleoperation-to-autonomy conversion box that would fit inside one of the three payload bays, complete with an Intel *Dual Core* processing board, KVH *DSP-3000* fiber-optic gyro, MicroStrain *3DM-GX2* IMU, with USB and Ethernet connectors. Small enough to fit into all the tunnels that were explored, the *PackBot®* provided a robust wireless communication link without any additional radios attached. The *PackBot®* is 52 centimeters wide x 89 centimeters long x 17 centimeters tall (no payload).

Figure 7. *PackBot®* with mounted NREC *MultiSense-SL*.

3.2.2 RoboteX® *AVATAR® II*

The RoboteX® *AVATAR® II* is a smaller alternative platform to the *PackBot*® but offered many of the same capabilities at a much lower cost (Figure 8). If the primary user of these systems is the Customs and Border Protection, under current fiscal conditions the costs of the entire package would have to be reduced significantly. This platform served as a mitigation effort for that risk. The biggest concern with this platform was that it had been designed for teleoperation only and was not ready for autonomous control. SSC Pacific engineers worked with RoboteX® to design a solution for an integrated controller that would accept commands for velocity, rotation, flippers, and camera rotation, which had previously only been available strictly from RoboteX®'s handheld controller. Integration with the embedded radios on the *AVATAR® II* was not feasible, so wireless communications required an additional radio attached to the platform. Wireless control and perception-sensor integration of this platform was demonstrated in November 2013 at the demonstration and test near the international border of California south of San Diego (Section 9.2). The *AVATAR® II* is 38 centimeters wide x 61 centimeters long x 15 centimeters tall (no payload).

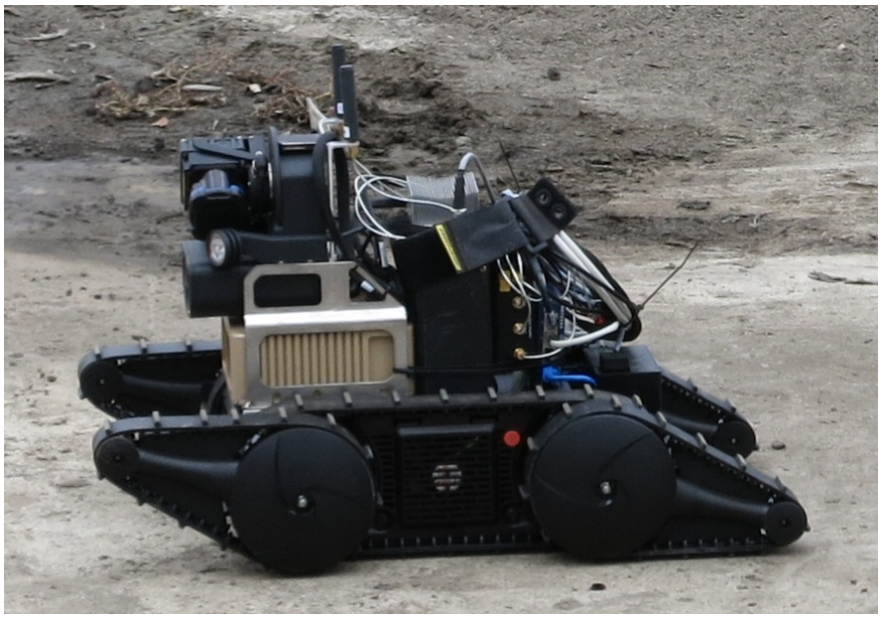

Figure 8. *AVATAR® II* mounted with sensors and radios.

3.2.3 Unmanned Aerial Vehicles

The use of aerial vehicles was outside the scope of the *Counter Tunnel* effort, but based on experiences gained in the evaluation, it would be worth exploring their use in tunnel environments. Based on prior work completed by the University of Pennsylvania [6] and some innovative methods of quadrotor protection demonstrated with the Laboratory of Intelligent Systems' *GimBall* [7] or the Illinois Institute of Technology's *Hytaq*, this method could provide a quick and efficient way of traversing and mapping tunnels. Research conducted by the Jet Propulsion Laboratory and University of California (UC) Berkley demonstrates the capability to add the required sensors on board a quadrotor and to ingress through a small rectangular opening like a window [8]. The potential advantages of an air vehicle are further reinforced by issues encountered during a data collection of a cross-border tunnel where the *PackBot*® was continually jarring up and down from the makeshift push-cart tracks, which introduced error into the localization solution (see Section 9.3). An aerial vehicle could fly through the tunnel and collect the data without the jerky

movements. These days, prices for quadrotors and their autopilots have come down significantly and can be purchased for less than $1000 from companies such as UAir or 3DRobotics.

4. COMMUNICATIONS

4.1 COMMUNICATIONS REQUIREMENTS

The communication requirements of the *Counter Tunnel* project included controlling the UGV for a distance of 400 meters while it traversed through a tunnel that had two 45-degree turns and an additional 90-degree turn. The effective communications range in tunnel applications depends on several factors that fall into two categories: radio characteristics and environmental factors. The radio characteristics of greatest importance are power emitted, RF channel bandwidth, frequency, and antenna selection. The environmental factors are distance of the antenna from any of the tunnel surfaces and size, shape, curvature, and material composition of the tunnel. The system-specific constraints include space allocated for the radio, Ethernet interface, and power usage.

The environmental factors are difficult to model for all given possibilities; hence, to encompass the variability of tunnel environments, testing occurred at multiple tunnels chosen to represent the breadth of tunnel variability that the system could experience.

4.2 RADIO SELECTION TESTING

The radio-selection test tunnel was chosen based on adherence to the anticipated environmental factors that the system would experience. The propagation effects of the tunnel were tested to determine the cutoff frequency and ideal operating frequency.

SSC Pacific engineers chose a tunnel in the Twentynine Palms area which had approximate dimensions of 1.5 meters tall by 0.9 meter wide (Figure 9a). The test site was an old mining tunnel, built by hand, representative of the target environment. Frequency sweeps were performed with wide-band logarithmic antennas at heights of 0.9 meter and 0.3 meter respectively at various distances (Figure 9b). A plot of the results is shown as amplitude vs. frequency in Figure 10. Additional tests were conducted at the Eagle mine in Julian, CA (Figures 12a through 12c). The cutoff frequency for this test was 600 MHz, with an optimal frequency of approximately 1 to 1.3 GHz. These results guided the initial radio selection.

4.3 RADIO SELECTION

The chosen radios that meet the initial space allocation and power usage were Silvus *4x4 MIMO* radio at 2 watts and 1.3 GHz, Trellisware *Wildcat II* unit at 8 watts at 1.8 GHz, and Cobham *Mini-IP* radio at 2.4 GHz (the 1-GHz version was unavailable).

4.4 RADIO TESTING

The radio testing consisted of transmitting 1 Mbps of data from the distant node to the base station that would simulate video data. The distant node was also transmitting approximately 80 Kbps of data that would simulate command and control data. The base station antenna was approximately 0.9 meter off the ground, while the distant node antenna was approximately 0.3 meter off the ground. SSC Pacific engineers conducted the tests at the Twentynine Palms test mine and the Julian Eagle Mine. The Twentynine Palms test mine included one distinct 45-degree bend. The maximum range results of the selected radios at Twentynine Palms were as follows: Trellisware - 122 meters, Cobham - 106 meters, and Silvus - 100 meters,

(a) (b)

Figure 9. (a) Twentynine Palms test mine opening. (b) Antenna used in the communication test at Twentynine Palms test mine.

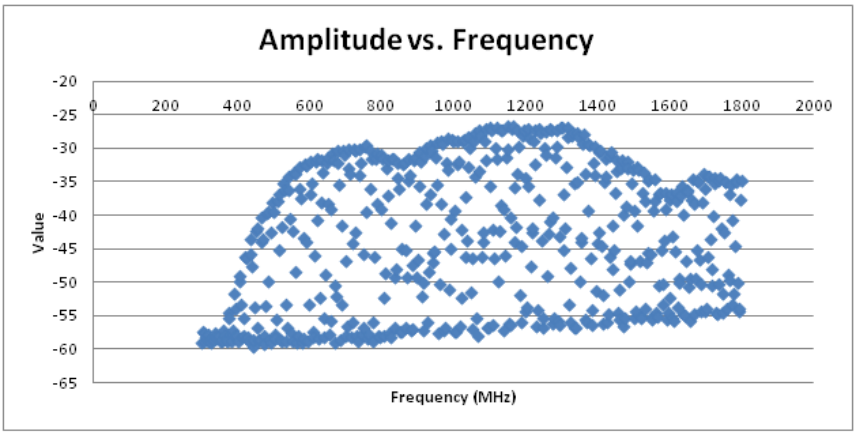

Figure 10. Plot of amplitude vs. frequency for wireless communication tests.

(a) (b) (c)

Figure 11. (a) Silvus radio, (b) Trellisware radio, and (c) Cobham radio.

respectively. The Julian Eagle Mine (Figures 12a through 12c) is a tunnel with a 91-meter straight section followed by a 90-degree turn with an additional 30-meter section, followed by an additional 90-degree turn. All three radios maintained communications for 122 meters at the Julian mine, which included the two 90-degree turns. However, the Trellisware radio traversed an additional 1.8 meters after the last bend.

(a) (b) (c)

Figure 12. (a) Entrance, (b) tunnel, and (c) shoring of the Eagle Mine in Julian, CA.

4.5 RADIO DOWNSELECT

The testing results did not provide a substantially superior radio solution. The Trellisware radios required a purchase of 10 radios due to production costs, which was prohibitive. Alteration of the space allocation during the manufacturing process for the *CTER* made the Silvus Radios no longer a feasible option. The tested Cobham radios were on loan and did not operate at the optimum frequency. Hence, engineers assumed performance of these radios would improve at the alternate frequency and this solution was chosen.

5. PERCEPTION

The *Counter Tunnel* project had perception requirements to localize the egress points within a meter of accuracy after traversing 400 meters without Global Positioning System (GPS) and to create a 3D model of the tunnel environment for obstacle avoidance, characterization, measurement, and analysis. A 3D model is especially important for obstacle avoidance because the tunnel environment is so varied, consisting of stairs, rocks and debris, rail and cart system, etc. This perception sensor design task was fulfilled by the National Robotics Engineering Center (NREC) with their prototype 3D sensor system, now called the *MultiSense-SL*.

5.1 PERCEPTION SENSOR

SSC Pacific chose the National Robotics Engineering Center (NREC) as the contractor to develop the prototype 3D sensor system to meet the localization and mapping requirements in a small package. After evaluating various perception sensors such as flash lidar, time of flight (TOF) lidar, phase shift lidar, scanning radar, stereo cameras, and structured light, NREC chose to develop a combined TOF lidar and stereo camera sensor.

Figure 13. NREC *MultiSense-SL* perception sensor includes a rotating lidar, stereo cameras, and strobing LED lights.

The *MultiSense-SL*, Figure 13, uses an axially spinning Hokuyo *UTM-30LX-EW* rotating about the z longitudinal axis, an optimal view for tunnels, which is calibrated with the left camera of the stereo pair.

Four strobing LED lights surrounding the sensor provide enough lighting for accurate stereo camera analysis in no- or low-light conditions, such as inside a tunnel. The software (a hardened computing box with an Intel *Core i7* processor) computes the position estimate through visual odometry (VO) from the stereo cameras at 10 Hz and a position correction from the iterative closest point (ICP) algorithm from the lidar at 3 Hz. On a side note, teams competing in the Defense Advanced Research Projects Agency (DARPA) Robotics Challenge (DRC) in track B and C used this sensor; DRC track B and C teams competed in a software-only challenge where winners received funding and an assignment of the Government furnished Boston Dynamics *Atlas* robot with a *MultiSense-SL* sensor head.

SSC Pacific's tests demonstrated that the *MultiSense-SL* provided an accurate 3D point cloud representation of indoor and outdoor environments, tunnels, buildings, and lab spaces (see Figures 14 and 15). However, because visual odometry is the primary localization method used, position estimation becomes noisy and cannot recover when it has no visual features to detect or track (e.g., within a few centimeters to a wall).

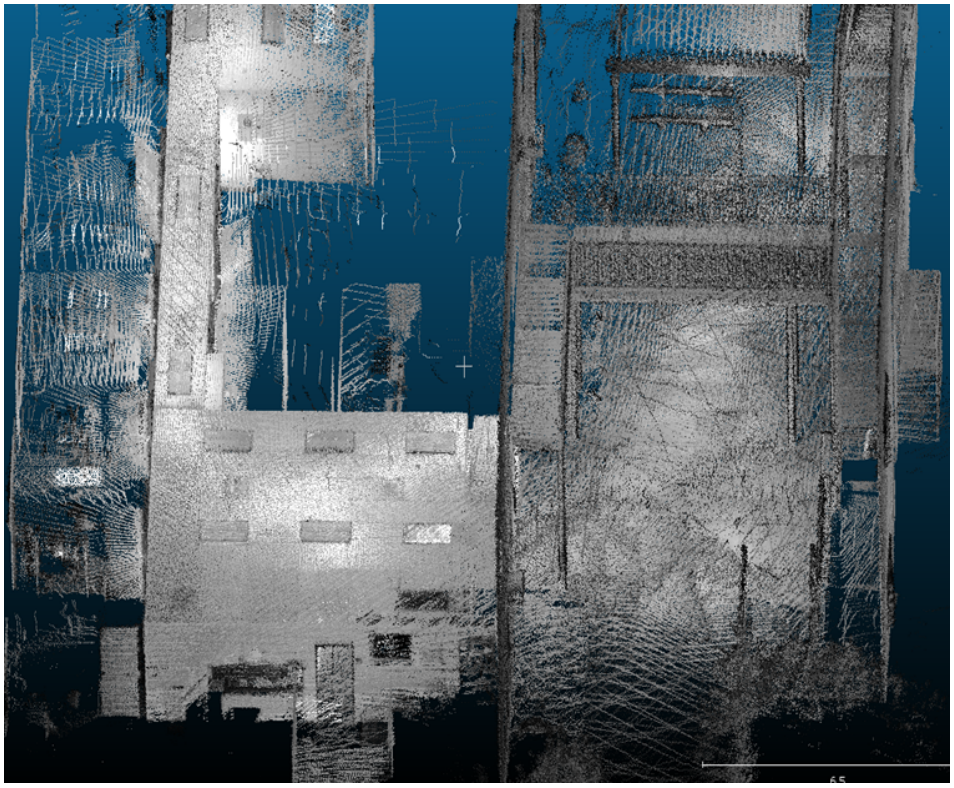

Figure 14. Top-down view of a point cloud of lab buildings, captured and stitched together from the *MultiSense-SL* sensor.

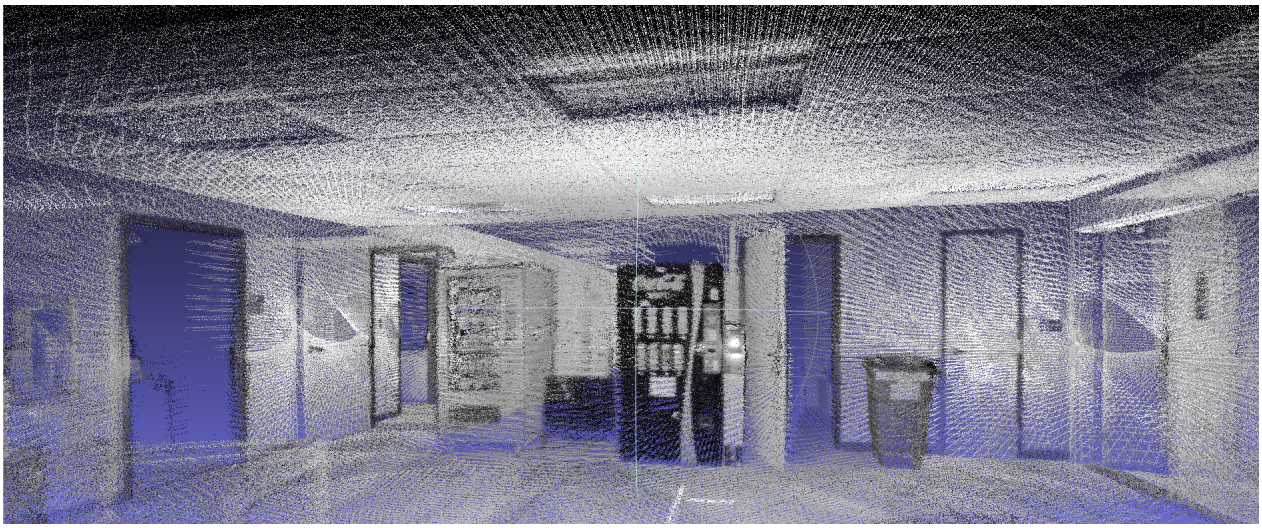

Figure 15. Point cloud of lab space, captured and stitched together from the *MultiSense-SL* sensor.

6. LOCALIZATION AND MAPPING

The robotic vehicles operating inside a tunnel must perform in a GPS-denied environment, mapping, localizing, and providing a georeferenced position of the egress points at more than 400 meters from the entry with a maximum error of 1 meter. This performance level requires accurate measurements and tightly coupled solutions to the localization problems. The diagram in Figure 16 illustrates the challenges for the whole system: GPS readings will be captured at the entry point of the borehole; the orientation, angle, and distance of the Borehole Deployment/Retrieval Apparatus needs to be calculated while moving through the borehole; the vehicle must localize itself with respect to the Borehole Deployment/Retrieval Apparatus once it has been deployed; and finally the vehicle will need to accurately calculate its odometry through the tunnel.

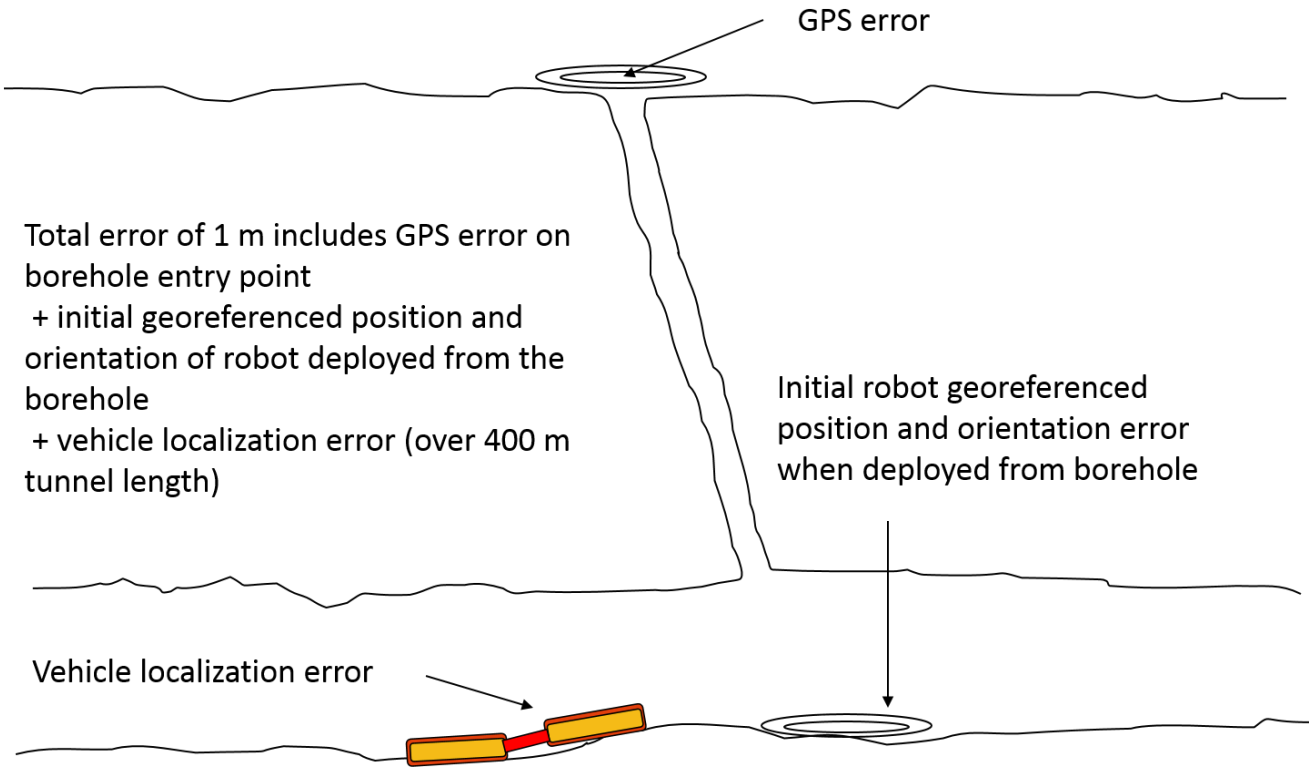

Figure 16. System localization error.

6.1 BOREHOLE APPARATUS LOCALIZATION

One of the challenges in creating an accurate georeferenced 3D map of a tunnel is obtaining an initial geospatial location and orientation. This initial pose anchors the 3D map in reference to known locations on earth and without an accurate estimate, the projection of the tunnel and most particularly the exit points may have a high degree of error. The majority of geospatial location devices use GPS, but the tunnel environment, which may be as much as 30 meters below the surface, prevents GPS units from functioning effectively due to the weak signal received at those depths. SSC Pacific needed to find a positioning system that can take a geospatial position while on the surface of the borehole and calculate the change in position as the delivery capsule descends through the borehole. The position system also had to meet certain technical specifications that are described in Table 2, showing the comparison of the specifications of

the desired versus the chosen system. The unit meets all the specifications was the Kearfott *KI-4901 T-24* inertial navigation unit (INU).

Table 2. Kearfott INU specifications versus requirements.

Specification	System Requirement	Kearfott *KI-4901 T-24 INU*
North Finding Capability	Yes	Yes
Position Accuracy	$\leq$ 0.5% of distance traveled, CEP	$\leq$ 0.1% of distance traveled, CEP
Orientation Accuracy	$\leq$ 1.0 mils (1 sigma)	Heading $\leq$ 1.0 mil Roll/Pitch 0.5 mils
Unaided Alignment Time	$\leq$ 30 min.	$\leq$ 15 min.
Temperature Range	-40 °C to 55 °C	-40 °C to 55 °C
Allowable Dimensions	0.154 m diameter x 0.406 m length	IMU: 0.114 m diameter x 0.160 m length CCA: 0.133 m length x 0.108 m width x 0.018 m depth

CEP = Circular Error Probable
IMU = Inertial Measurement Unit
CCA = Circuit Card Assembly

The Kearfott *KI-4901 T-24* INU is composed of an inertial measurement unit (IMU), a Circuit Card Assembly (CCA) that contains the processor and support electronics, and a power supply and DC-DC converter. Prior to alignment, the Kearfott INU requires a position input, which can be provided using GPS or through a geodetic survey over the center of the borehole at surface level. Once the Kearfott INU receives the known position, normal alignment begins. With the unit stationary, the alignment process takes 15 minutes before pose information is available. Detection of excessive motion on the Kearfott INU halts alignment. Once aligned, navigation can proceed. Since no GPS position updates will be available when the capsule goes down the borehole, the INU is solely responsible for calculating the capsule's current pose. Due to the gyro drift and accelerometer bias errors growing over time, Zero Velocity Updates (ZUPT), initiated whenever the capsule is stationary, need to be performed to keep the pose accuracy within limits.

6.1.1 Kearfott Accuracy Test Results

Prior to using the Kearfott INU for calculating the RDC reference initial pose, the INU was benchmarked for accuracy. The accuracy test results showed that the unit performed to specifications.

The accuracy tests revealed that using the default Zero Velocity Update (ZUPT) interval of 30 seconds gave the best results for both 2D and 3D position accuracy as well as orientation accuracy. When operators did not use ZUPTs, pose solutions drifted to the point of being unusable. Constraining the rotational movement of the capsule during borehole traversal provided a tighter pose solution. The data from these tests are presented in Table 3.

6.1.2 Borehole Insertion Testing

Prior to borehole insertion, the Kearfott INU had to perform alignment after receiving an initial GPS position, a process that took 15 minutes to complete. The long alignment period makes it crucial to avoid capsule movement during the process. Once aligned, pose data was collected when the capsule was at home position prior to movement; at ZUPT stop positions; and touching the bottom of tunnel floor. The

Table 3. Kearfott accuracy test data (azimuth, pitch, and roll measurements are in degrees).

Test Run	Duration (min)	Distance (m)	ZUPT interval (sec)	2D error	3D error	dAzimuth	dPitch	dRoll
Static2	39.48	0	30	0.000	0.000	0.006	0	0
Horizontal3	8.52	1090	NO ZUPT	118.991	119.310	0	0.141	0.056
Horizontal6	32.00	1090	30	0.074	0.080	-0.011	-0.118	-0.073
Horizontal4	14.88	1090	60	0.080	0.100	-0.006	-0.051	-0.017
Horizontal5	12.33	1090	120	0.296	0.296	-0.005	0.029	0.022
Vertical1	6.51	28	NO ZUPT	15.213	15.974	0	0.422	0.309
Vertical5	31.31	32	30	0.323	0.356	-0.022	-0.371	0.321
Vertical6	23.25	26	60	0.199	1.841	-0.006	-0.14	-0.371
Vertical3	23.78	40	120	0.843	0.849	-0.005	0.709	0.377

difference in horizontal position (latitude and longitude) from the home position to the tunnel floor position during testing was 4 millimeters. The total vertical travel calculated by the INU was 3.52 meters compared to the 3.5 meters reported by the winch encoder. A 6-degree change in the yaw was attributed to the capsule experiencing minor rotation as it went down the borehole. Roll and pitch values varied by 0.3 degrees.

6.2 FIDUCIAL LOCALIZATION

Once the vehicle deploys from the Borehole Deployment/Retrieval Apparatus, it localizes itself with the apparatus, which has already localized with the surface coordinate system (normally GPS). The vehicle does this by first detecting the exposed portion of the deployment apparatus using a rotationally invariant localization fiducial attached to the tip of the apparatus (Figure 17). References for this technique are in [9] and [10]. With the known size and pattern of the localization fiducial, the vehicle can then calculate its six degrees of freedom position and orientation using only a single image from a single camera. This position and orientation can then transform through the known apparatus coordinate frame to localize the vehicle with the surface coordinates.

6.2.1 Fiducial Pattern

The localization pattern is composed of black or white circles inscribed within oppositely colored black or white squares. This allows the pattern to contain binary data as well as be easily localized using calibration techniques. In the cylindrical case, the encoded data can encode the yaw rotation of the pattern as viewed from different vantage points. In the flat case, the bits can encode the unique identification of the pattern, allowing large-scale localization with multiple patterns. In either case, the pattern needs to be rotationally unique, e.g., no rotation of the pattern can equal itself or any other pattern. In the cylindrical case (Figures **??** and 19), every view of the pattern needs to be rotational unique. If this uniqueness discontinues, localization ambiguities will arise, allowing for multiple possible solutions. Ensuring that the patterns are greatly different from each other allows for some additional error checking. To achieve this critical uniqueness, the targets use a solid strip of black or white circles on the bottom and an alternating pattern on top (Figure 20).

Figure 17. Deployment of the *CTER* platform through the Borehole Deployment/Retrieval Apparatus with attached localization fiducial.

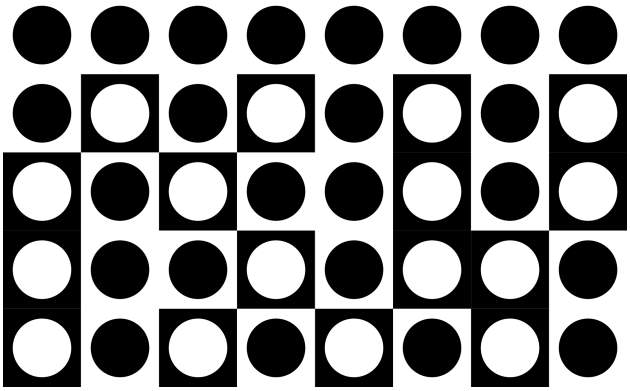

Figure 18. 5 x 8 cylindrical fiducial pattern.

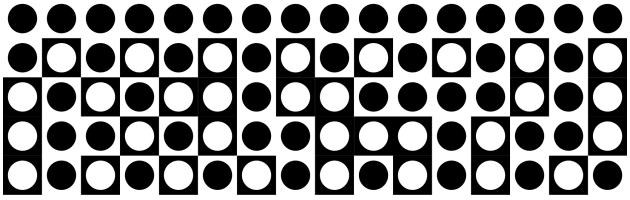

Figure 19. 5 x 16 cylindrical fiducial pattern.

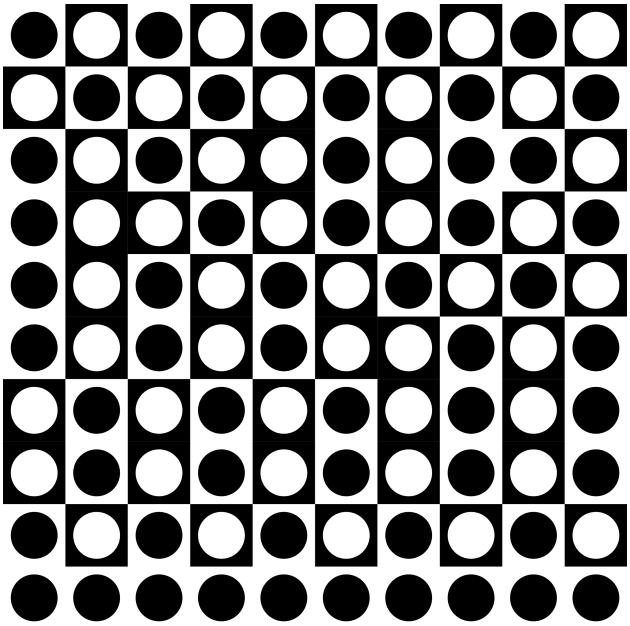

Figure 20. 10 x 10 planar fiducial pattern.

6.2.2 Localization Algorithm

The localization algorithm calculates the relative position of the origin of the image with respect to the pattern. The algorithm first detects possible bits using a contour detection algorithm. Contours detected between two threshold values and contours at multiple threshold levels, and which are sufficiently convex, are added as potential pattern bits. Figure 21 shows contour detection run on a cylindrical pattern. The values of the threshold minimum and maximum, as well as the threshold step, determine which intermediate threshold values are used. Larger ranges and smaller steps will make the detection algorithm more sensitive but take more time to process, whereas tighter ranges and larger steps will be faster but may miss some of the pattern bits. Once the potential bits are detected, they are clustered using hierarchical clustering over both location and contour diameter. The largest clusters detect the presence of a bit pattern and organize the bits into a grid structure.

The algorithm compares the grid to the pattern using different rotations and different shifts. Figures 22 and 23 illustrate matching on cylindrical patterns. In the cylindrical case, these shifts translate to rotations about the cylinder. The rotation and shift with the greatest number of fully matched columns is used for localization. In a cylinder, the columns are the only fully visible portions of the pattern. Ties are broken by the total number of bits matched. Perspective-n-Point camera pose estimation performs on the pixel locations and the matched patterns' 3D model points, resulting in a full six degrees of freedom transform from the image to the pattern. Mean reprojection error is used to break any remaining ties. When using multiple unique patterns, each potential pattern can be matched and ties can be broken as previously mentioned to determine which pattern matches best. This transform can be combined with the known global pose of the pattern to determine the global pose of the image. A brief overview of the algorithm is shown in Algorithm 1.

Algorithm 1 Calculate image pose using fiducial pattern.

Require: $Image, Pattern, Model, ModelPose$
  $ImageBits$:= BlobFinder($Image$)
  while $size(ImageBits) > 0$ **do**
    $BitsOfInterest$:= HierachicalCluster($ImageBits$)
    $Grid$:= DetectPattern($BitsOfInterest$);
    $[Mapping_{Grid \to Pattern}, ColumnMatches, BitMatches]$:= FindBestMatching($Grid, Pattern$)
    if $ColumnMatches > MaxColumnMatches$ **or** $ColumnMatches = MaxColumnMatches$ **and** $BitMatches > MaxBitMatches$ **then**
      $MaxColumnMatches := ColumnMatches$
      $MaxBitMatches := BitMatches$
      $[ImagePose, ReprojectionError] = PnP(Grid_Bits, Mapping_{Grid \to Pattern}, Model)$
    end if
    $ImageBits := ImageBits - BitsOfInterest$
  end while
  $ImagePose := ImagePose + ModelPose$
  return $ImagePose, ReprojectionError$

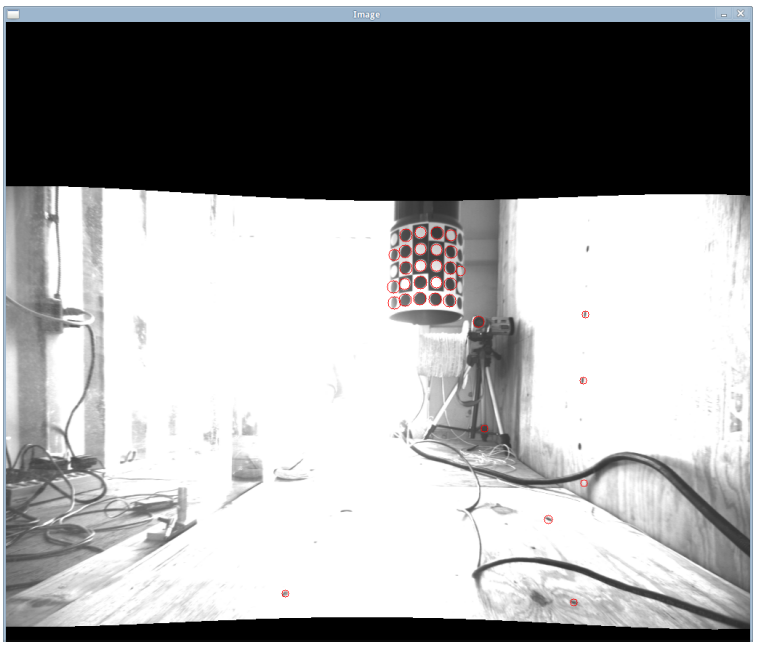

Figure 21. Contour detection on cylindrical fiducial pattern in mock tunnel.

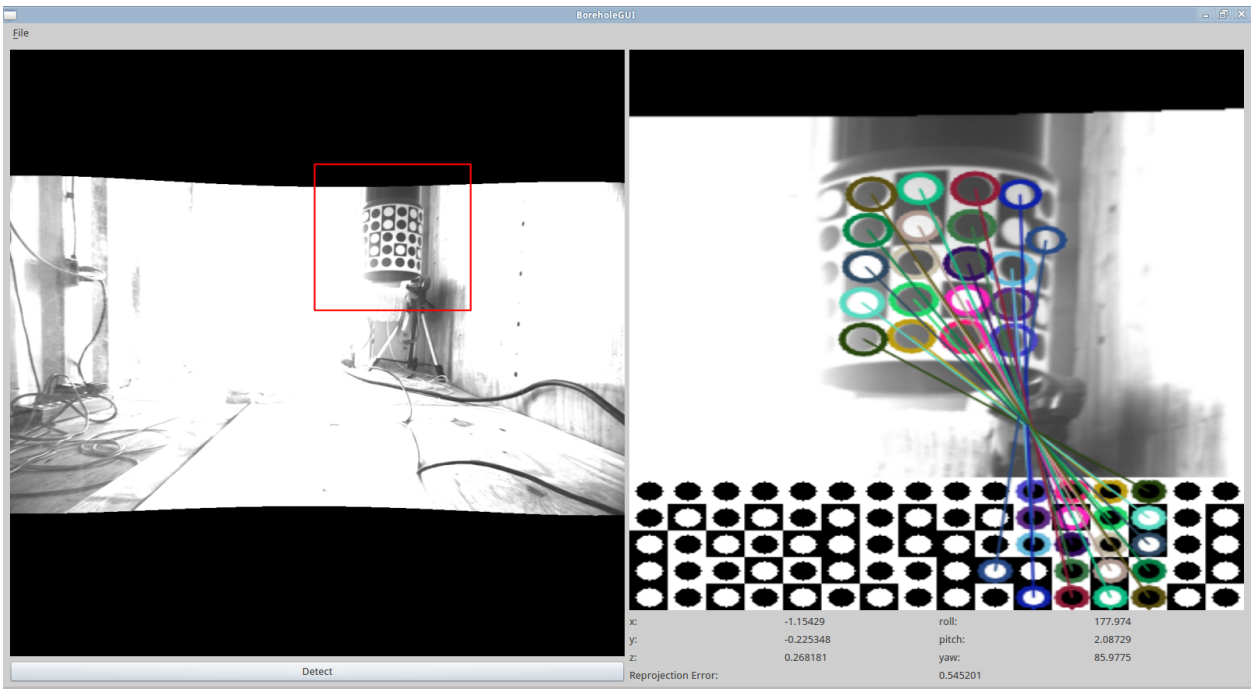

Figure 22. Fiducial matching to a cylindrical pattern.

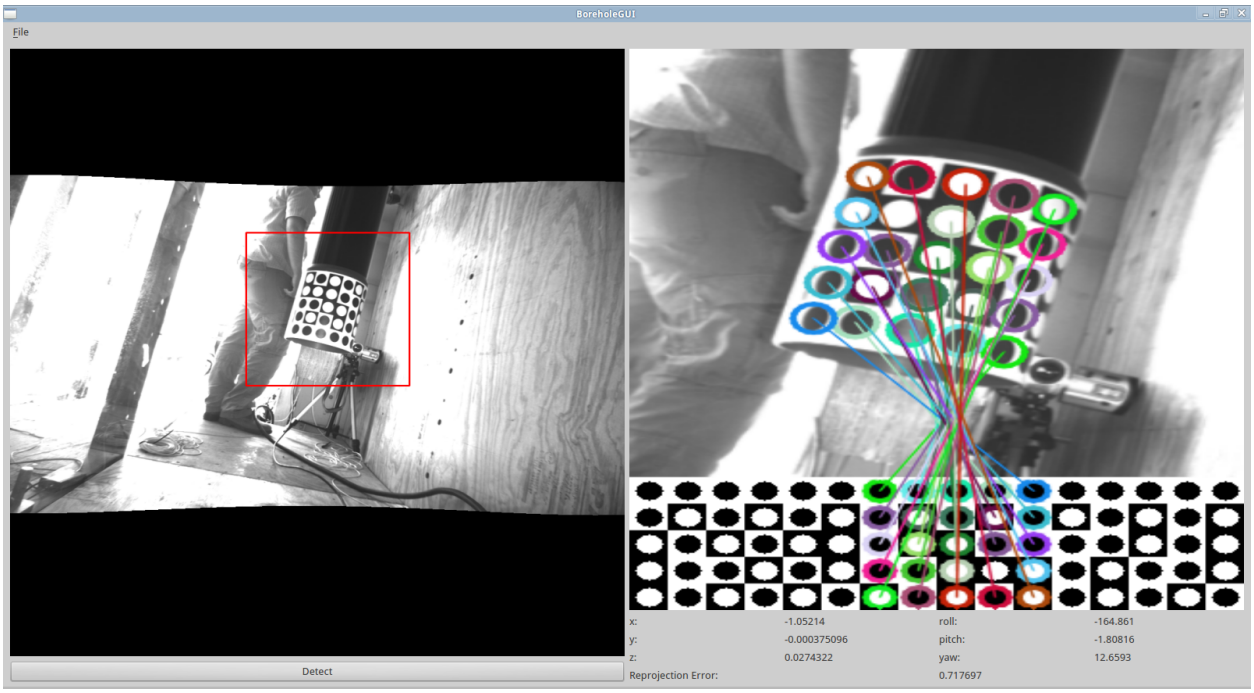

Figure 23. Fiducial matching to a tilted cylindrical pattern.

6.2.3 Fiducial Localization Testing

Tests of this method produced results that were within 1- to 3-centimeter accuracy and less than 1-degree azimuth angle error. These results were determined using the camera images from the *MultiSense-SL* and the lidar scans from the same sensor as ground truth. The authors postponed more thorough testing of the fiducial system to implement an April Tags [9] solution for comparison. However, time and budget restrictions did not allow for additional localization implementations or more thorough testing.

6.3 VEHICLE LOCALIZATION

The *MultiSense-SL* was designed to provide perception and localization for the system, but when the *CTER* platform and the *MultiSense-SL* sensor were delivered, integration testing showed significantly degraded mobility performance. The *CTER* platform was very unstable with the NREC sensor mounted on the arms of the front tracks, often causing tip-over. A second generation of sensor miniaturization was planned but didn't go forward due to budget cuts. During testing, engineers used the *Roll* mode to self-right the platform after tip-over, but the drive gear of a bender joint broke a tooth due to the weight of the sensor and the robot went back for repairs. Due to this instability, localization and mapping tests were conducted solely with the *PackBot*® platform and not on the *CTER*. An alternative 2D simultaneous localization and mapping (SLAM) solution was tested in parallel.

6.3.1 *MultiSense-SL* Localization

Localization tests conducted with the *MultiSense-SL* sensor mounted to the *PackBot*® platform produced positive results. The localization from the sensor is produced from the visual odometry algorithm from the stereo vision cameras and corrected with an ICP algorithm from the lidar data. No formal characterization of the accuracy of the localization of the *MultiSense-SL* sensor was performed due to budget and time issues. SSC Pacific ran an informal test of the sensor mounted on a *PackBot*® multiple times inside a 1.5-meter-diameter concrete storm drain, driving 450 meters in and 450 meters out (a total of 900 meters traveled), including a bend of 90 degrees, and the x,y-position error after returning to the original location (based on *MultiSense-SL* odometry only), was 0.9 meter. This was an impressive feat, especially because the visual features in a concrete storm drain are sparse, as shown in Figure 24. The storm drain with a manhole access point can be seen in Figure 25a and as a registered point cloud in Figure 25b.

6.3.2 Alternative 2D Mapping Localization

The *CTER* platform could not safely manage the weight of the *MultiSense-SL* without becoming unstable and tipping over, so AFRL developed a 2D mapping system using a Hokuyo *UTM-30LX* lidar mounted on the *CTER* (Figure 26) and used SLAM open source software *Hector Mapping*, found in the Robot Operating System (ROS). The test setup and test are described below.

6.3.2.1 2D Mapping Test Setup. AFRL performed the mapping test using a Hokuyo *UTM-30LX* scanning laser mounted on the *CTER*. The sensor data was passed to a laptop running ROS (Robot Operating System) and using *Hector Mapping* for SLAM. *Hector Mapping* is a method to perform SLAM using only a horizontal lidar scan and no odometry information. A 9- to 36-VDC to 12-VDC converter supplied power to the Hokuyo using a 25-VDC lithium-ion battery stored in the front track compartment of the *CTER*. The battery prevented extra power draw on the *CTER* and thus extended the range of the robot.

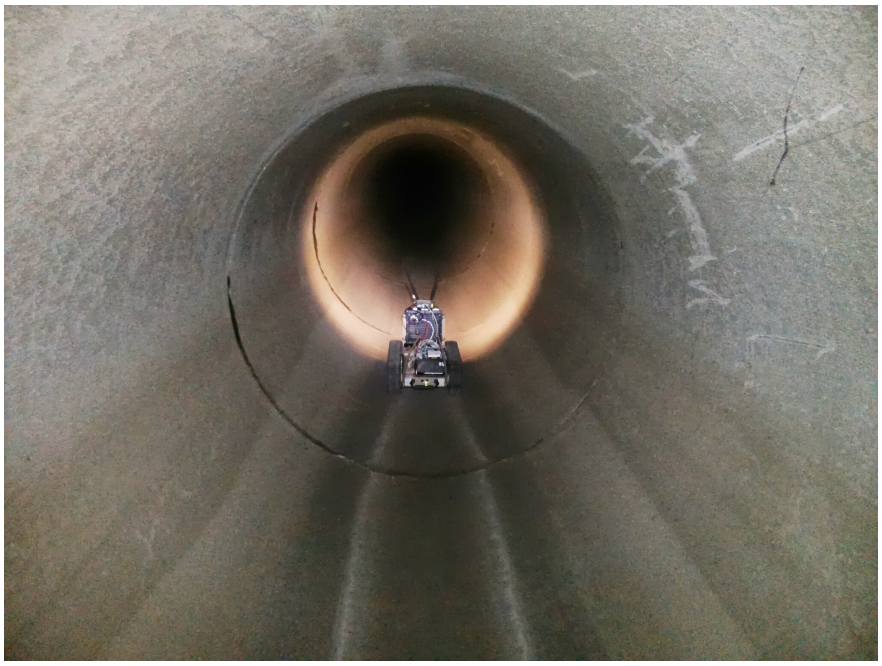

Figure 24. *MultiSense-SL* mounted on a *PackBot®* mapping and localizing in a concrete storm drain.

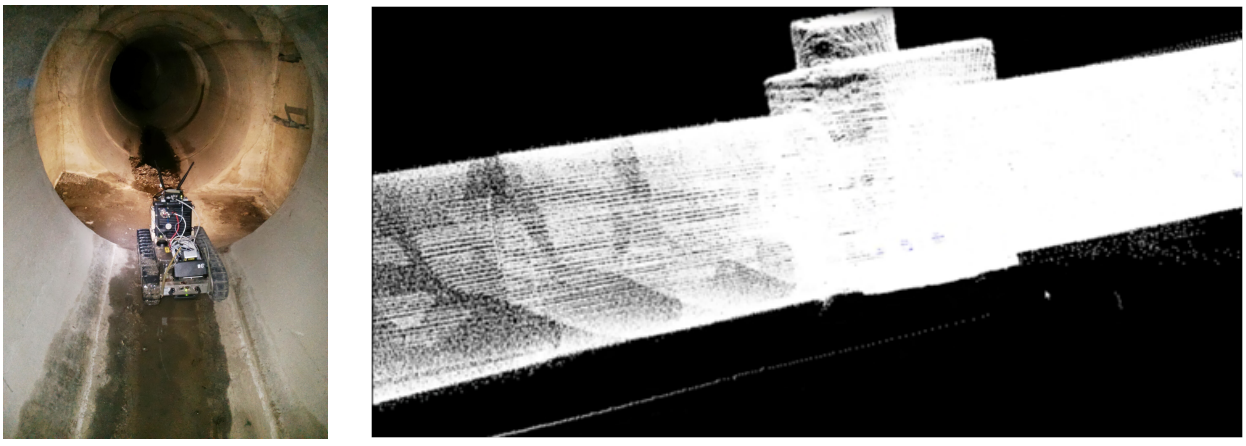

(a) (b)

Figure 25. (a) An over-the-shoulder view of the *PackBot®* in the storm drain pipe with a manhole access point. (b) A registered point cloud of the same manhole as perceived by the *MultiSense-SL*.

Figure 26. *CTER* platform with mounted Hokuyo lidar sensor (lower left).

AFRL performed two tests with the 2D sensor. For the first test, the *CTER* and mounted sensor were loaded on a cart and pushed manually around the robotics fabrication facility. This test verified operation of the sensor mounted on the snake, and ensured the SLAM software worked properly. For the second test, the *CTER* was teleoperated through a mock tunnel.

6.3.2.2 2D Mapping Test Results. The initial test of the sensor was performed by pushing the *CTER* on a cart to verify operation was successful. This test verified that battery life was sufficient to keep the sensor running for at least as long as the *CTER*'s endurance. Also verified were proper operation of the computer and software that were performing SLAM based on the laser scanner data. This test included large open spaces, office spaces, and various equipment and obstacle features. The interior layout of this building allowed for a loop to be made inside of the building. While it was known prior to this test that *Hector Mapping* does not perform loop closure, it proved to be accurate enough for most situations. The lack of loop closure was evident during this test, as loops around the fabrication facility resulted in errors as seen in Figure 27.

AFRL performed the second test of the sensor in a mock tunnel environment. This test highlighted the issues of using 2D mapping for this application. The test run was a single loop around the test tunnel. The mock tunnel had sections of smooth concrete walls, walls with regularly spaced supports, and walls with random rock, wood, and trash features. The floor variations included smooth concrete, crushed rock, dirt, and sections of 91-centimeter culvert (concrete, steel, and PVC). Aluminum covered the top of the non-culvert portions of the mock tunnel. These varied terrain features simulated multiple types of tunnels that Border Patrol officers, law enforcement, or warfighters may encounter during counter-tunnel operations. Ensuring that the sensor was facing forward was essential during this test. Since there was no angular feedback on the *CTER* front arms (laser mounting location), this had to be set prior to running the test. The specular aluminum ceiling of the tunnel caused reflections and inaccuracies in the reported distance of the laser scans. It was also very evident that *Hector Mapping* was not sufficient for mapping areas with smooth walls or regularly spaced supports. Figure 28 shows the SLAM output became confused while mapping these types of surfaces. The *Hector Mapping* SLAM algorithm determined that the robot had not

Figure 27. Lab facilities map created by *Hector Mapping* with errors from loop closure.

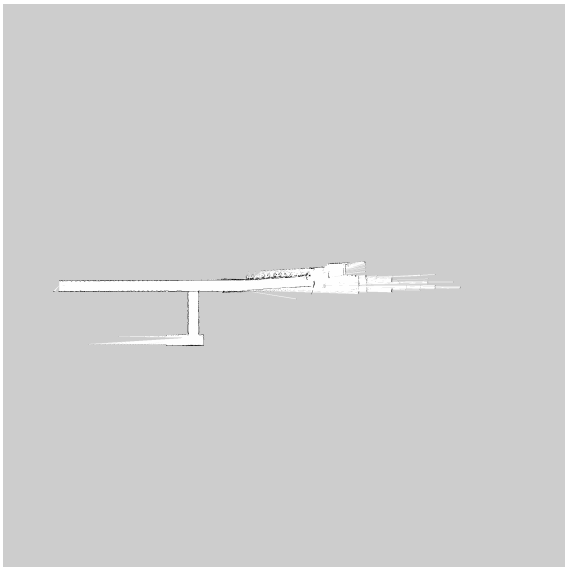

Figure 28. Localization error (an obstacle was placed across the left-turn entrance) from *Hector Mapping* due to the featureless smooth walls in tunnel.

moved, when in reality it had, and updated the map showing a wall across the entrance to a turn to the left. This misinterpretation was due to the wall not having sufficient features for the laser to distinguish.

6.4 SLIDE IMAGES

SSC Pacific explored the use of slide images, a tunnel-based point descriptor algorithm, which uses the central axis of the tunnel to construct a radial histogram of the tunnel walls, as a method of loop closure and initial localization. This histogram provides a frame-independent feature, because it is calculated relative to the central axis as opposed to a synthetic coordinate system. This approach requires the central axis of the tunnel be estimated from the available point cloud data. Once estimated, the point data around each portion of this axis is segmented and binned to calculate the histogram. More information concerning this technique is found in [11] and [12]. In Figure 29, a small portion of tunnel, shown in blue, was used to estimate the central axis, shown in red. This segmented data, shown in green, produces a series of slide images. Using the gravity vector as another frame-independent reference point (shown in green in Figure 30), the distance from the axis (the length of the red vector) and the angle about the axis (the angle between the green and red vectors) were used to bin the individual points. This histogram was then blurred, using a standard Gaussian kernel, to dampen the effects of noise in the point data. Figure 31 shows a completed slide image with the y-axis bins showing the angle about the y-axis and the x-axis bins showing the radius from the central-axis.

SSC Pacific tested a localization estimation using slide images against an iterative closest point (ICP) algorithm initialized using the centroids of the point clouds. The slide image algorithm performed significantly better (results shown in Figure 32), mainly because it does not rely on an initial guess transform. However, when the ICP algorithm was initialized close to the correct solution, it out-performed the slide image algorithm. It was determined that the slide images would make a better initialization algorithm, whereas ICP would be used as the primary registration algorithm. In addition to initializing registration, the slide image could be used for volumetric analysis of the tunnel structure, integrating the cross-sectional area over the tunnel axis. One of the problems with the slide image representation is its difficulty in han-

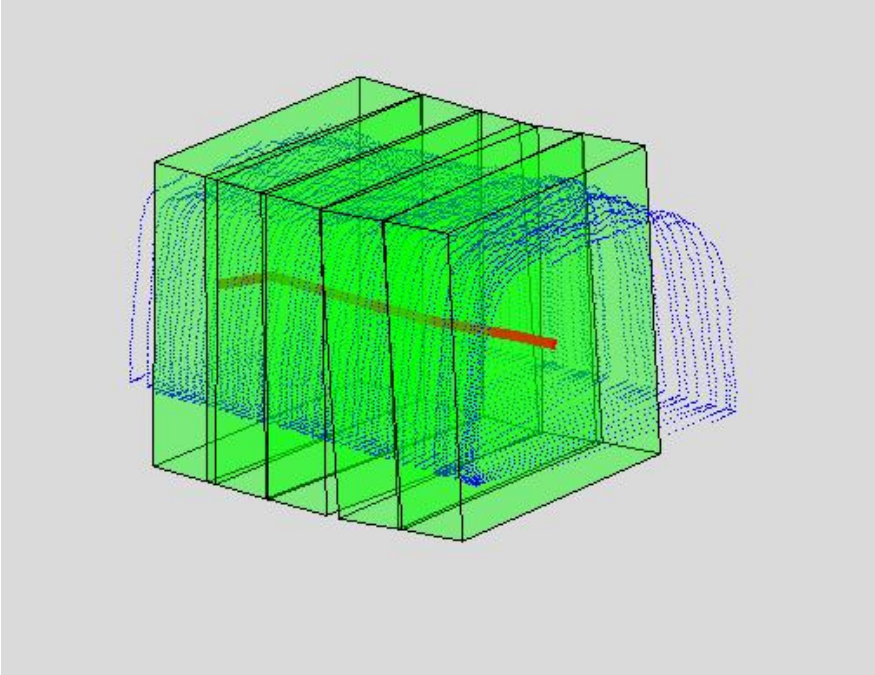

Figure 29. Scan segmentation for slide image generation.

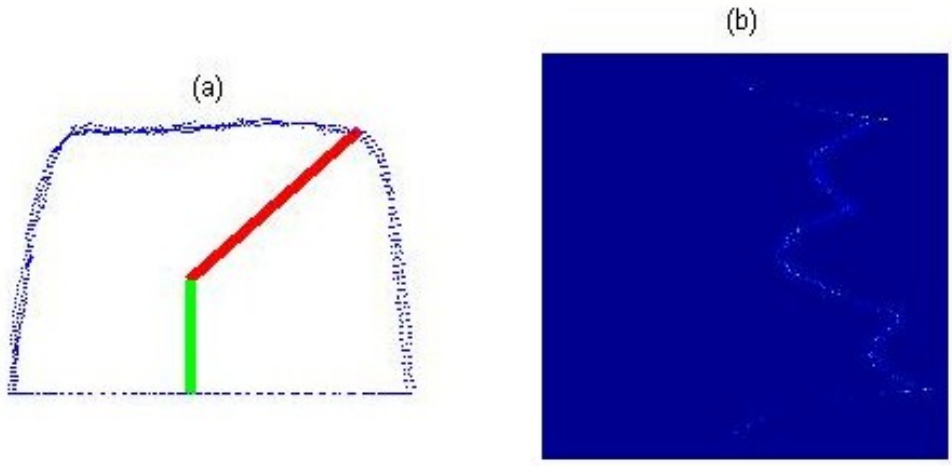

Figure 30. Slide image histogram generation: (a) tunnel segment with point and gravity vector, (b) standard 2D histogram.

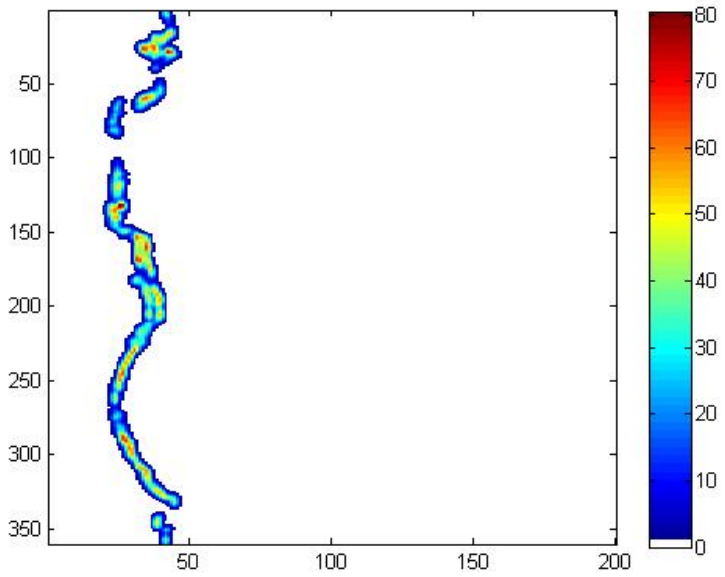

Figure 31. Gaussian blurred slide image histogram.

dling intersections where the axis is ambiguous. This problem could be solved using a graph-based axis instead of the purely linear one. These algorithms were implemented and tested using lidar scans from border tunnels using the SSC Pacific's *Nodding Hokuyo* lidar, a prototype design for mechanically rotating the Hokuyo *UTM-30LX* horizontal laser scanner along its y-lateral-axis to collect a full 3D point cloud.

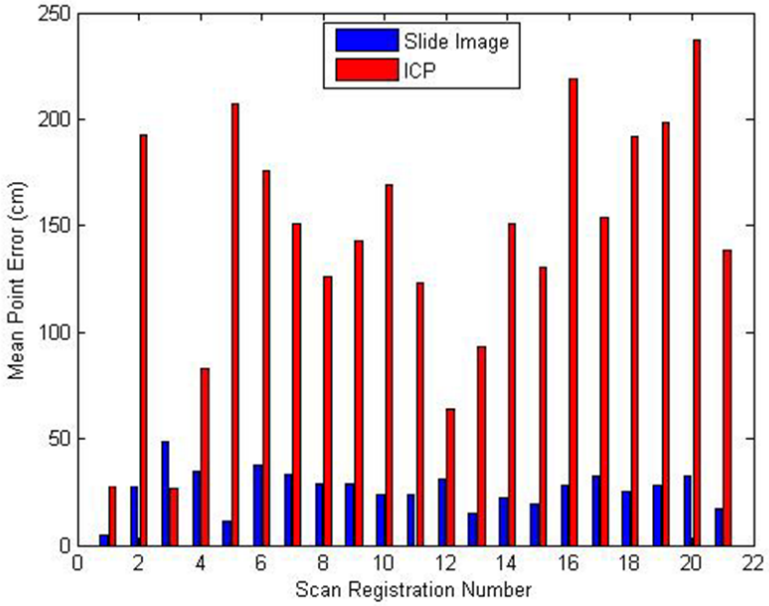

Figure 32. Accuracy of uninitialized ICP and slide image pair-wise registration; data capture from *Nodding Hokuyo* lidar in border tunnel.

6.5 STRUCTURE FROM MOTION

Additional localization and mapping efforts were performed using structure from motion (SfM), a range imaging technique that estimates 3D models from 2D images, such as from a camera. This technology finds correspondences between images, tracking them over multiple images, which then reconstruct the feature 3D positions and the motion of the camera. This technique provides a 3D model, although with a scale ambiguity. The SfM capability was leveraged from the SSC Pacific *Urban Environment Modeling (UrbEM)* project, which uses the same technology found in Microsoft's *PhotoSynth* [13]. *UrbEM* was a development effort focused on autonomously building rich 3D models of urban environments from a ground perspective, to be used for path planning, mission planning, and training for warfighters, along with localization for moving robotic platforms. A sample image from a data collection in the cross-border Marconi tunnel is shown in Figure 33, with an image of the 3D model in Figure 34.

Figure 33. Cross-border Marconi tunnel steep downward steps.

Figure 34. Cross-border Marconi tunnel 3D reconstruction.

7. AUTONOMY

It became apparent that this project would need basic autonomous capabilities such as traversing the tunnel while avoiding obstacles and creating and updating a map for the user. Not only would wireless communications be intermittent at a distance of 400 meters away from the base station, but it tends to be hard on the operator to teleoperate a vehicle through a narrow tunnel for such a long period of time. SSC Pacific engineers decided to use the *Autonomous Capability Suite (ACS)*, an advanced autonomous behaviors architecture that can be used for navigation, mapping, and exploration in various indoor and outdoor settings, to satisfy the needs of this project.

7.1 SOFTWARE: *AUTONOMOUS CAPABILITY SUITE (ACS)*

SSC Pacific engineers had previous experience using the *Autonomous Capability Suite (ACS)* for autonomous funcionality integrated on the *PackBot*® with other SSC Pacific projects. This architecture provided integration of navigation sensor drivers and perception data through the SSC Pacific *CommonSense* libraries, and navigated autonomously through various indoor and outdoor environments [14].

The obstacle avoidance software in *ACS* was designed for a single-scan lidar, so software modifications were necessary for the vehicle to function with NREC's 3D sensor. The limitations of computing power on-board the *CTER* robot made it infeasible for the obstacle avoidance algorithms to work in 3D space during normal operations and unnecessary for most of the time in the tunnels. However, the 3D point clouds made it possible to measure the height of objects lying in the path, detect overhangs, or classify slopes and determine if these objects were indeed obstacles for a specific robotic platform. An algorithm was developed that simplified the 3D stitched point cloud into a two and a half dimensional (2.5D) obstacle grid that would provide height information about approaching objects, overhangs, and slopes. Each specific robotic platform could then react differently to objects in the path (e.g., the *CTER* could climb steps up to 30 centimeters in height whereas the *PackBot*® would avoid objects of 10 centimeters or greater). This 2.5D grid was merged into the *ACS* 2D obstacle map to provide simple path planning searches and obstacle avoidance.

Path planning was developed to explore goal points in areas the robot had not mapped before and plan appropriate paths to those locations. However, because of the simple linear shape of most drug-tunnels, autonomous navigation required only a simple open-space behavior. This behavior looks for space in front of the robot that is open, keeps itself centered between any obstacles on its left and right side, and creates a trajectory that moves it safely through that space. The user-assisted autonomous software mode allowed the user to provide suggestions of rotation (left turn, right turn) that would influence the behavior-based trajectory planning while the autonomous navigation would continue to avoid collisions.

8. *MULTI-ROBOT OPERATOR CONTROL UNIT (MOCU)*

The *Counter Tunnel* project added functionality to SSC Pacific's existing *Multi-robot Operator Control Unit (MOCU)* [15] to control both the *CTER* and the *PackBot*® platforms in a tunnel exploration mode by creating two new modules. One module was responsible for retrieving and displaying the obstacle map, while the other module was responsible for sending control messages and processing the video feed and vehicle's pose.

MOCU was configured to connect to the *Autonomous Capability Suite (ACS)* in order to receive the robot's pose and obstacle map data as well as to provide control. *MOCU* connected directly to the robot to receive the video feed. A display configuration was set up to allow the user to view a 2D map on the bottom left, a 3D terrain map on the right and a live video feed from the robot in the upper left (as shown in Figure 35). Robot control modes are selectable via an on-screen menu that is navigated via a gamepad controller. The menu allows the user to select the robot for control and switch between three control modes: *Guarded Teleop* (teleoperation that will not allow the user to hit obstacles), *Teleop* (pure teleoperation), and *Explore* (autonomous). As the robot is driven, *MOCU* overlays an obstacle map over the 2D and 3D maps.

MOCU leveraged a previously funded SSC Pacific effort with the Robotics Technology Consortium (RTC) partner Pelican Mapping which placed the georeferenced tunnel point cloud (collected from the sensors) in the map. Point-to-point measurement on the rendered scene for tunnel characterization model measurements was also implemented.

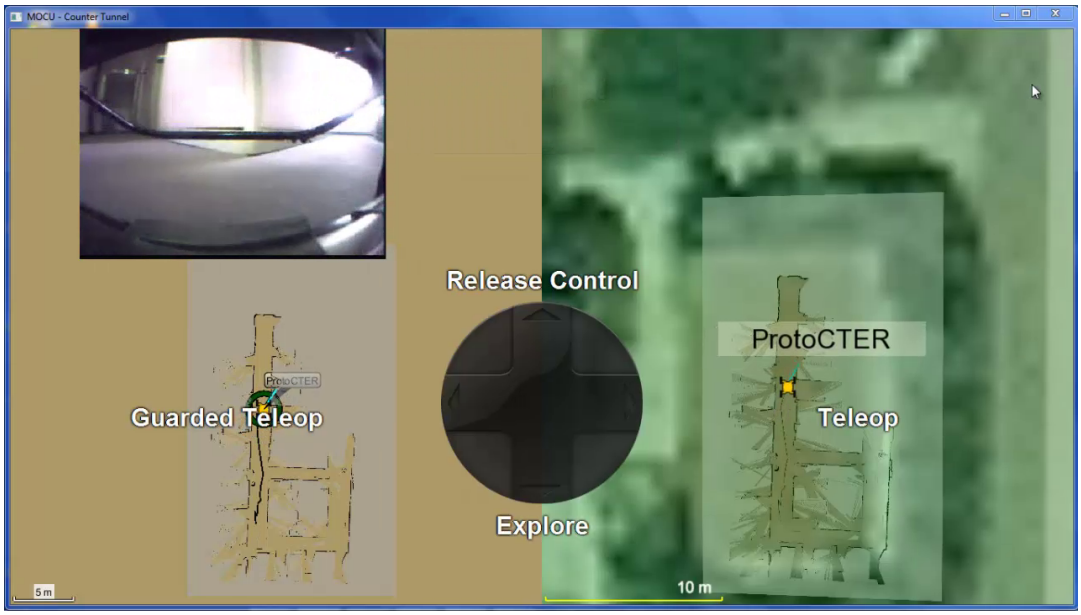

Figure 35. Screenshot of *MOCU* controlling a *PackBot*® in lab space with an obstacle map layered on top of both a 2D map and a 3D terrain map.

9. SYSTEM TESTING AND DEMONSTRATION

This project required a vastly different testing environment than the typical indoor or outdoor test sites used by most robotic programs. Finding an ideal testing location in itself was a difficult task, especially one that could provide a realistic environment in keeping with project objectives. The SSC Pacific project team visited various sites for autonomous robotic exploration, sensor data collection and analysis, and radio communication tests. The ideal test sites were the cross-border tunnels discovered by the U.S. Customs and Border Protection near the U.S.–Mexico border, particularly in San Diego. However, the timeline for testing in these tunnels was always short because the Border Patrol fills them in quickly with cement for safety and security reasons. Because of the lack of publicly available underground tunnels in the area, at one point during the project, SSC Pacific rented and tested inside a commercial mine in Julian, California (it is humorous to note the reactions from the SSC Pacific purchasing department when they reviewed a request to rent a gold mine for a government-sponsored activity). Because of the dangers of working in enclosed tunnel environments, SSC Pacific engineers worked closely with their safety office for training and preparing and using safety gear for site visits. Figures 36a through 36d display some of the testing environments that were visited.

(a) (b)

(c) (d)

Figure 36. (a) A tunnel test site in Twentynine Palms. (b) *PackBot®* maneuvering in a cross-border tunnel. (c) *CTER* maneuvering through a test tunnel (d) *PackBot®* maneuvering through a test tunnel.

9.1 JOINT AFRL/SSC PACIFIC DEMONSTRATION

A joint demonstration was held with AFRL and SSC Pacific in June 2013. The details of this event were approved with a Distribution Statement C, distribution authorized only to U.S. Government agencies and their contractors. To be able to receive approval for public release (Distribution A) for this report, the specifics of the June 2013 event have been left out. The demonstration included sensor data collection, mapping and localization within a tunnel, autonomous driving through various ground cover and wall texture environments, wireless communications with repeater nodes, deployment and retrieval of the *CTER* platform through the Borehole Deployment/Retrieval Apparatus, driving the *CTER* robot through various modes, as well as climbing up and scaling down 30-centimeter steps and crossing over 30-centimeter gaps.

9.2 DEMONSTRATION AND TEST WITH U.S. CUSTOMS AND BORDER PROTECTION

SSC Pacific held an additional test and demonstration event near the border of California and Mexico with the U.S. Customs and Border Protection in November of 2013, demonstrating control of a *CTER*, *AVATAR® II*, and a *PackBot®* platform through three concrete storm drains. Storm drain #1 was a 45-centimeter-diameter culvert with no turns and a length of about 10 meters. Storm drain #2 was a 1.5-meter diameter culvert with one 90-degree turn at 20 meters and more than 300 meters long. Storm drain #3 was a 1.5-meter diameter culvert with one 90-degree turn at 30 meters, another 90-degree turn at 150 meters, and a total length of 350 meters. Demonstration participants controlled the *PackBot®* through wireless communications using *MOCU*, displaying a video stream and overlaid local map data on satellite imagery. The smooth surface and relatively straight line concrete culverts acted as an RF waveguide for the wireless communications, with no significant multipath or occlusion issues. From the base station in storm drain #2, 802.11 wifi provided video from the robot to the user allowed control of the robot for up to 450 meters away.

Tests in storm drain #3 provided an opportunity to use repeater communication nodes for greater driving distances. As was expected from previous communications tests in other tunnel locations, the wireless signal was lost after the second 90-degree turn, about 150 meters from the base station. *Manually Deployed Communication Relays (MDCR)*, a variant of the *Automatically Deployed Communication Relays (ADCR)* [16], a proven and fielded communications product developed at SSC Pacific, provided repeater relay communication nodes that increased the wireless communication distance. A repeater node placed at the second turn provided strong communications to the *PackBot®* for the rest of the tunnel length, another 200 meters (Figure 38a). The autonomy system was able to successfully travel the full distance of the storm drain with user interactions only at the start and the halfway point when the vehicle turned around (Figure 38b). The Border Patrol Program Manager mentioned that the SSC Pacific autonomy running the *PackBot®* through the storm drains was "Border-Patrol-agent-proof," meaning that since it was hands-off autonomy, the operators could not break it.

The *AVATAR® II* was integrated and tested for wireless teleoperation and mapping with the *MultiSense-SL*. The *AVATAR® II* is shown with the Cobham radio for wireless communications and a *MultiSense-SL* in Figure 39. This platform performed with similar maneuverability as the *PackBot®* albeit with a smaller obstacle height with respect to the mud, rocks, and water found in the tunnels due to its low profile and smaller fins.

A test was conducted with the *CTER* platform through storm drain #1, shown in Figures 40a through 40c. The *CTER* platform was connected with fiber and controlled using the *CTER* control software with video and position feedback as shown in Figure 40b. The small diameter of the storm drain provided

(a)

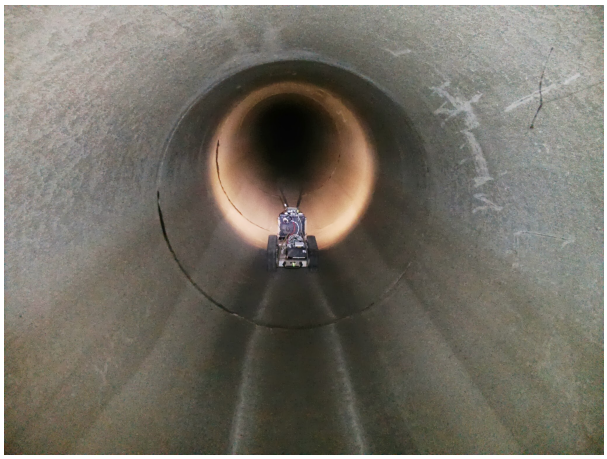

(b)

Figure 37. (a) Software engineer Jacoby Larson sends the *PackBot®* into a storm drain near the international border south of San Diego using wireless communications. (b) The *PackBot®* autonomously traversing and mapping the 1.5-meter concrete storm drain.

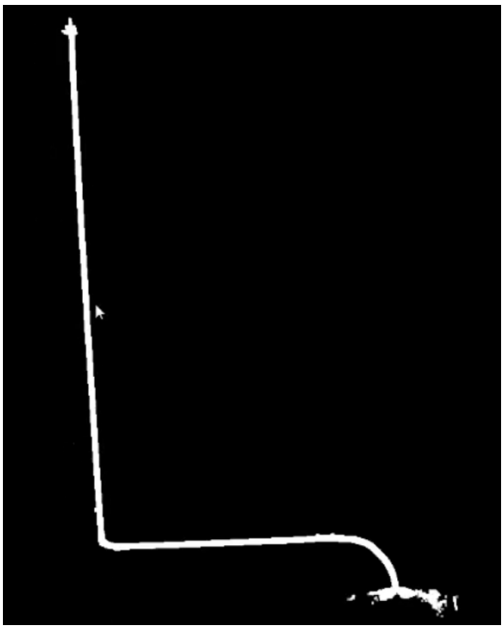

(a)

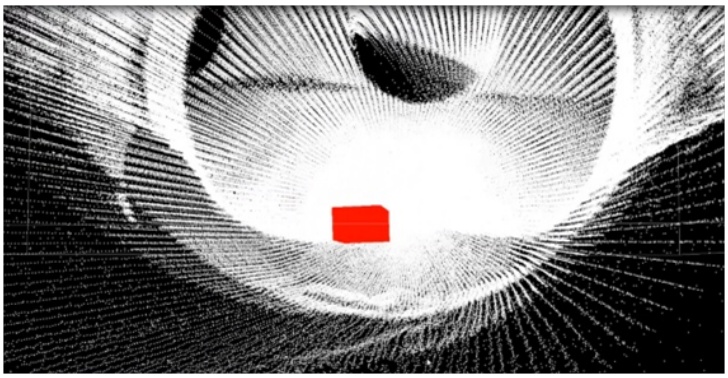

(b)

Figure 38. (a) Top-down view of a 3D point cloud of storm drain #3 near the international border south of San Diego, showing two 90-degree turns. (b) 3D point cloud of the end of the storm drain (the red box represents the location of the robot in the scene).

Figure 39. *AVATAR® II* robot equipped with sensors and radios about to enter a storm drain near the international border south of San Diego.

a very unstable surface for a single-track linear platform and the *CTER* consequently tipped over after traveling only 3 meters. The small width of the culvert made maneuvering and recovering from tipover very difficult, especially when only using video feedback. The test team attached an auxiliary supporting structure to the front track section, as seen in Figure 40c, which allowed the platform to successfully drive the remaining length of the concrete pipe.

(a) (b) (c)

Figure 40. (a) *CTER* platform about to enter a 45-centimeter storm drain near the international border south of San Diego. (b) The video feed from *CTER* platform as it traverses the storm drain. (c) The attached angled fins provides stability for the *CTER* while traversing the storm drain.

The SSC Pacific team conducted additional mobility tests with the *CTER* at another set of storm drains with varying degrees of ground cover: soft and moist dirt, loose sandy steps, and large rocky terrain (Figures 41a through 41c). The Border Patrol had tested other platforms at these test sites and stated that none of the robots could climb the loose, sandy steps. The *CTER* platform, with its unique control and maneuvering capabilities, was able to wriggle, rotate, and climb up the steps in its predefined *Bend* mode.

(a) (b) (c)

Figure 41. (a) *CTER* platform beginning to traverse sandy terrain in a storm drain at the international border south of San Diego. (b) *CTER* successfully traversed the sandy stepped terrain. (c) *CTER* in *Bend* mode traversing rocky terrain in another storm drain.

The Borehole Deployment/Retrieval Apparatus was not tested at this event, but feedback from the field operators was that it did not require much more effort or cost to dig a 60-centimeter borehole than a 20-centimeter borehole. This 20-centimeter borehole requirement was the main driver for developing a new and extremely narrow platform, which had significant negative impact on cost, schedule, integration, and testing.

9.3 DATA COLLECTION OF CROSS-BORDER TUNNEL

The U.S. Customs and Border Protection provided support for a data collection at a drug-smuggling tunnel between the U.S.–Mexico border, discovered in November 2013, linking warehouses in San Diego and Tijuana. U.S. Customs and Border Protection normally secures such a tunnel, drills boreholes from the ground surface down into the tunnel, and fills it with concrete so that it cannot be reused. SSC Pacific was asked to map the tunnel and provide a set of GPS drilling points.

At the time of testing, ventilation in the tunnel was being set up and the air quality was unknown past 150 meters into the tunnel, which meant that an unmanned platform would be the only safe way to map the tunnel. One of the largest risks in this endeavor was that if the unmanned system failed to respond while in the tunnel for some reason (poor communication, broken motors, thrown track, etc.), it would be extremely difficult to retrieve.

The tunnel was equipped with a rail and cart system (Figures 42a and 42b) that made driving with the *PackBot*® only possible without front flippers (the flippers were too wide for the robot to fit inside the rails). An illustration of the robot configuration is shown in Figure 43. The tunnel was not wide enough for

the robot to turn around, so retrieval of the robot required that it be driven in reverse. The initial test was conducted with the robot driving 150 meters over the tracks with one repeater node placed at 75 meters for communication. Results from that test showed that the hard impacts of the vehicle lifting up and falling down over the cross ties caused a great deal of noise in the localization measurements and created a useless map of the tunnel.

(a) (b)

Figure 42. (a) Rail and cart system in a cross-border tunnel discovered by the Border Patrol. (b) Supporting cross ties for the rail system (the rail is on the left).

A cart was conveniently left in the tunnel and another test was conducted with the robot riding on the cart. This test would only be able to travel as far as a human operator could push the cart. Because of concerns for air quality, this was believed to be about 150 meters. However, when this test was conducted, the air quality sensors reported that the air in the tunnel was within acceptable health limits far beyond that length. The robot took a ride on the cart for 300 meters to the end of the tracks where the tunnel took a 90-degree turn to the left. From this point, the air quality sensors were at their threshold for safety and the robot was sent on its own. The base station was set up at this turning point and the robot was driven an additional 150 meters over another set of tracks, which were also very bumpy. At a distance of 150 meters, the communication was poor and the vehicle was driven backwards to the turning point and the test was completed.

The map created from the *MultiSense-SL* was registered correctly up to the turn and provided a good representation of the tunnel, shown in Figure 44. No wheel odometry sensors were used during this test because the robot rode on the push-cart. The position of the robot in the tunnel was determined using only perception system sensors and the visual odometry and iterative closest point algorithms. To be able to provide accurate georeferenced drilling points for this tunnel, the point cloud had to be merged with a point cloud that had an accurate representation of the outside world. This was accomplished using a number of very dense point clouds collected with a FARO *Focus3D* system, stitched together using spherical fiducials, seen in Figure 45.

The overlap of the two point clouds was not significant and no fiducial markers were set inside the main tunnel body, so that merging of these point clouds together was accomplished by hand using open-source 3D point cloud and mesh processing software called *CloudCompare*. This hand registration introduced alignment error, where even a small error here could propagate into large position errors further down the 300-meter tunnel.

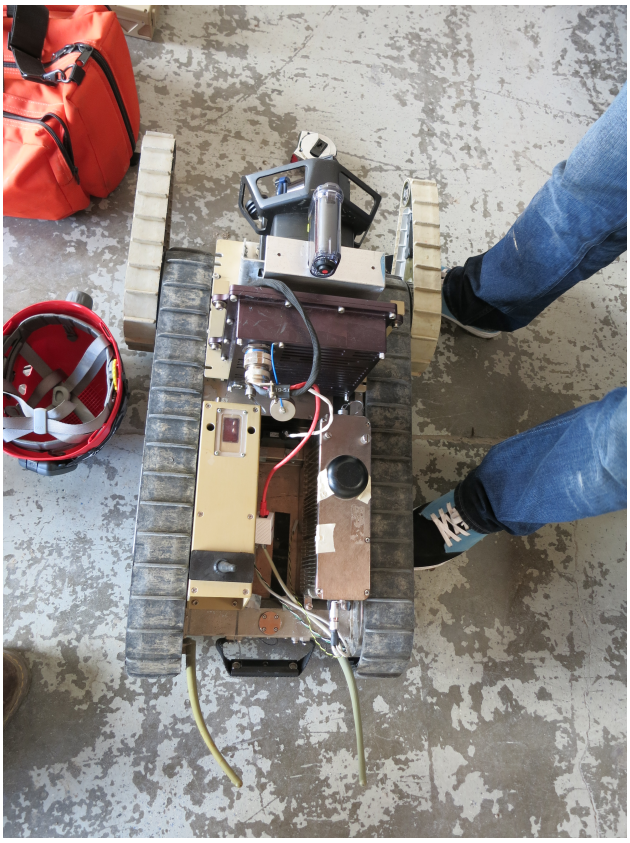

Figure 43. *PackBot®* with mounted 3D sensor, perception computer module (black box behind sensor), autonomy module (silver box on right rear), and radio communications module (tan box on left rear).

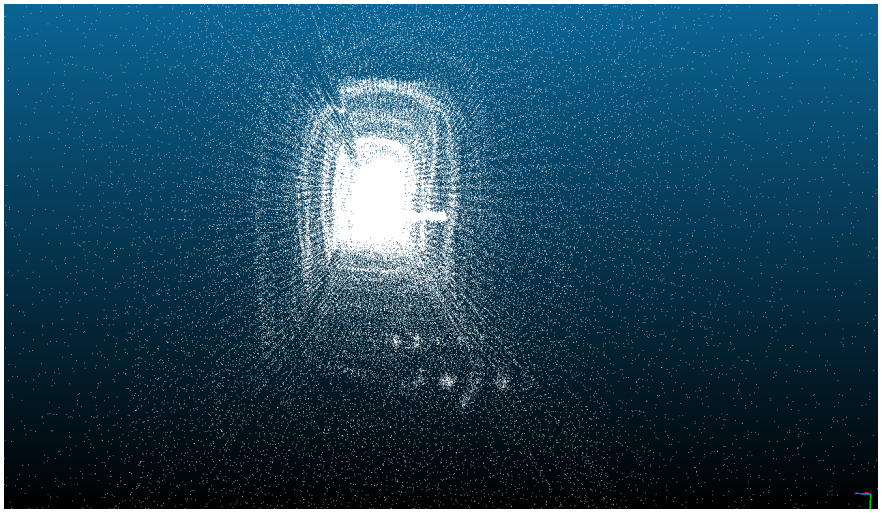

Figure 44. Point cloud of tunnel, captured from the *MultiSense-SL* sensor.

Figure 45. Point cloud of steps leading down into the tunnel, collected by the *Focus3D* sensor. Two of the spherical fiducials used to stitch scans together can be seen on the left.

This merged point cloud was then merged with a georeferenced top-down aerial lidar collection of the San Diego area from the USGS 2005 San Diego Urban Region Lidar data set. Every point in this USGS aerial point cloud has a NAD85 (HARN) state plane zone 6 coordinate which can be converted to a GPS coordinate. Once more, this aerial point cloud data set was merged with the tunnel data set by hand, which introduced more error, but provided a GPS reference to the tunnel. An illustration of the overhead view of the final point cloud is shown in Figure 46. Estimated GPS points were extracted from the tunnel every 15 meters (Figure 47) and provided to the U.S. Customs and Border Protection agents in a KML file for easy access in *Google Earth*^{TM}.

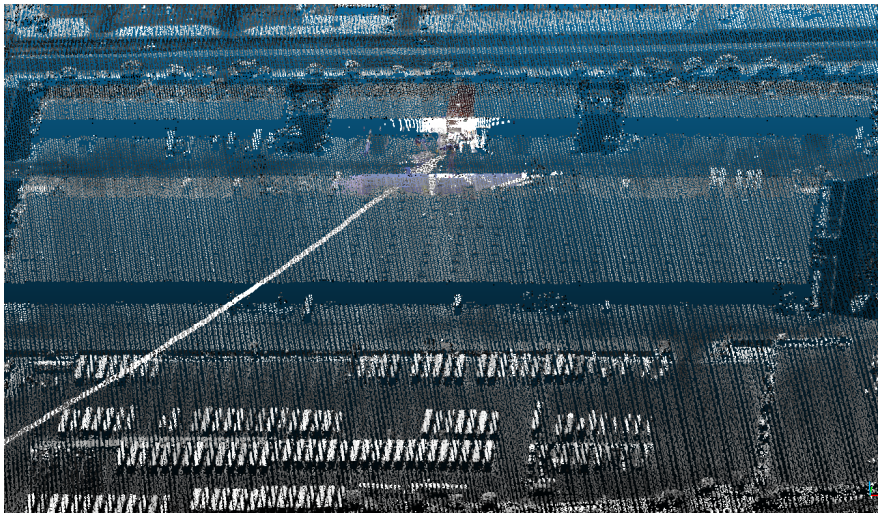

Figure 46. Point cloud of tunnel and warehouse merged with aerial lidar point cloud.

It was unclear at this point exactly how much error might have been introduced in the hand merging of point clouds. There was no reference point provided that could be used to bias the information. After drilling was completed, a KML file of actual drilling points was created to compare with the estimated drilling points of the tunnel. An image of the estimated and actual drilling points are shown in Figures 48

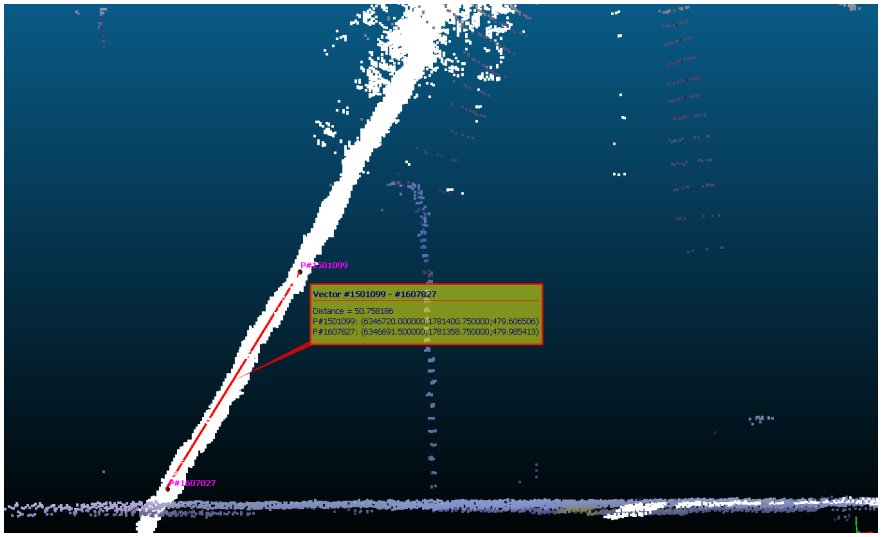

Figure 47. Overhead view of point cloud of tunnel with selection of drilling points every 15 meters.

and 49. The direction of travel of the merged point clouds by hand turned out to be accurate. However, the largest source of error was the estimated distance of the tunnel. The actual distance of the tunnel from the warehouse to the turning point was 336 meters but the final estimated tunnel length in the point cloud was 275 meters, an 18% error in distance.

The cause of the error in the distance was afterwards determined to have been a flaw in the *CloudCompare* software. As multiple point clouds were inserted into the program, they had to be merged together by rotating and translating the sets so they fit into each other. It was discovered that the multiple rotations of the tunnel point cloud, when merged with the warehouse point cloud, caused the tunnel to decrease in length. The tunnel started out as a point cloud that measured 308 meters, but after multiple rotations in the program, was measured to be only 265 meters. This was the final point cloud that was used in the GPS drilling point estimations and this change in distance was not discovered during the process. A test was later conducted and as the point cloud was rotated the tunnel distance was observed to decrease in size from 308 meters, 285 meters, 265 meters, down to 222 meters. After discussions with the developers of *CloudCompare* about the issue, it was discovered that the computations of the rotations were made with standard 32 bits (float) precision and the solution was for them to use double-precision matrices in the rendering pipeline. They have since made the change in their software and further tests reveal that the length of the point cloud now remains the same after multiple rotations.

This test showed that although there were some flaws in the method used to combine 3D point clouds and provide georeferenced tunnel points, those flaws have been identified and there is an immediate and huge potential for this technology to be used for newly discovered drug-smuggling tunnels. As this was the first time the SSC Pacific team had georeferenced the point clouds with GPS without using the designed borehole tunnel and fiducial apparatus system, this process was time-consuming and introduced some errors. This method could be refined and better automated with additional work and provide a more accurate and safer method for mapping tunnels and providing drilling locations where air quality and other conditions make it dangerous for humans.

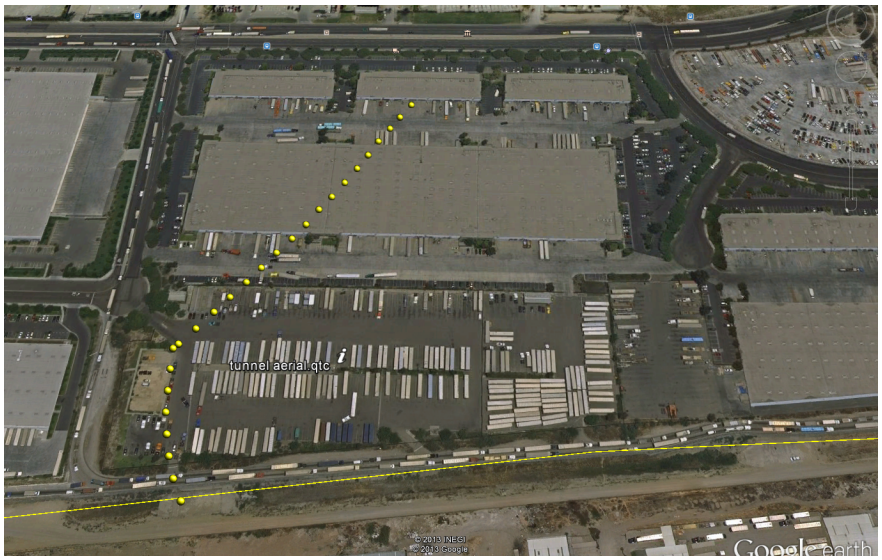

Figure 48. *Google Earth*™ image with overlayed estimated drilling points.

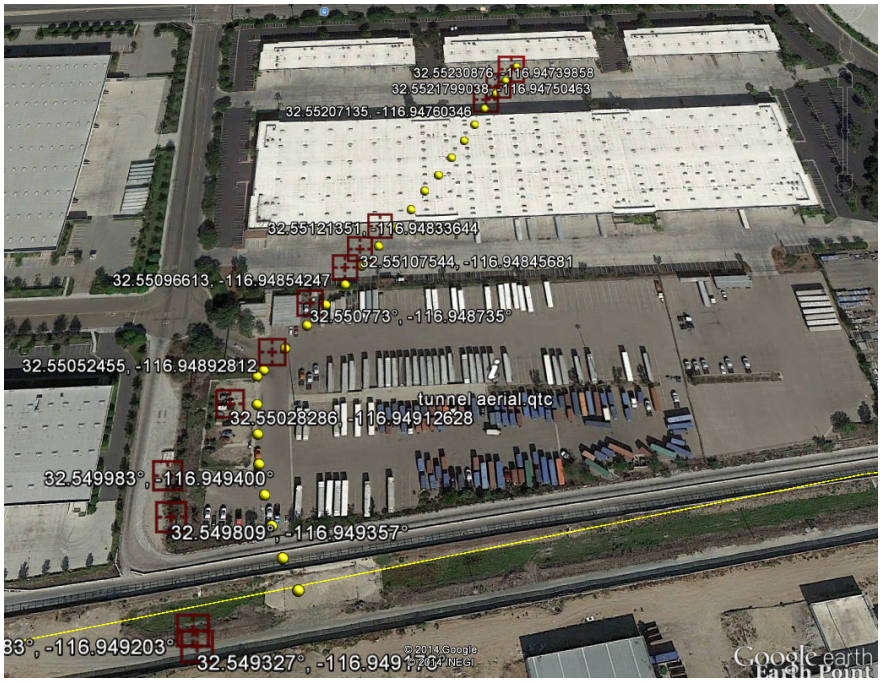

Figure 49. *Google Earth*™ image with overlayed estimated (yellow dots) and real drilling points (red squares).

10. FUTURE WORK

The *Counter Tunnel* project has explored a wide range of technologies and advanced the resultant capabilities needed for counter-tunnel exploration and mapping. Additional work is required to transition these technologies to the agencies that will put them to use in day-to-day activities for improving security and removing humans from danger. We recommend the following efforts.

Primarily, an investigation into the costs associated with drilling wider boreholes could have the largest impact. The 20-centimeter borehole requirement drove the design for the prototype mobility robot, the smaller perception sensor, and the specialized Borehole Deployment/Retrieval Apparatus, which increased cost and risk. This cost and risk might be prohibitive to the government agencies working in tunnel environments. If an investigation reports that a larger borehole (such as 60 centimeters) is not cost prohibitive (brief discussions with Border Patrol agents indicated this was the case), it could create a pathway for robotic platforms, larger than 20-centimeter width, and a more affordable and reliable solution. If the borehole diameter requirement cannot be changed, the following efforts would provide the greatest return on investment.

It is recommended to further miniaturize the perception sensor so the *CTER* platform will not tip-over from the sensor weight. Additional effort could be used to make the perception solution more robust to quick rotations or a lack of visible texture (such as when the sensor is within centimeters to an object, like a wall). Future work should integrate other sensor data (wheel odometry, gyroscope, accelerometers, or an IMU) with the data from the *MultiSense-SL* sensor to more robustly estimate the position and register the point clouds.

There is a need to perform another iteration of improvements for the *CTER*. Linkages, reliability, and insufficient torque should be addressed. Further modeling and algorithm development is needed to improve the *Anti-Roll* mode of the platform, especially when it is carrying heavy payloads.

The Borehole Deployment/Retrieval Apparatus was designed to meet the tight localization requirements associated with deployment down the borehole shaft 30 meters deep, and it met those requirements using a high-end IMU. If the Borehole Deployment/Retrieval Apparatus is to be used in the future by government agencies, there is a need to provide accurate localization with a cost-effective solution. This could involve additional sensors and/or an improved borehole localization algorithm.

Further research in the use of quadrotors or some small UAV platform for simple exploration and mapping inside tunnels is recommended. Typically these quadrotors have a battery life that only provides 10-15 minutes of flying time, but if the mapping and flying maneuvers are fast and accurate, 10 minutes would be sufficient to fly 800 meters through a tunnel and collect data. A UAV would also reduce the amount of effort that would be needed to traverse all of the various terrain that a robot encounters inside tunnels: dirt, debris, standing water, mud, stairs, steep slopes, etc.

Continued efforts are needed for UGV tunnel terrain traversability. Solving problems like how to drive over a rail and cart system inside a tunnel without continuous jarring up and down or climbing to the top of steep stairs without tip-over could be an avenue for research that would provide near-term improvements.

There is a need for improved methods of georeferencing tunnels to GPS coordinates. The data collection through the border tunnel in December 2013 demonstrated that it is currently possible to determine this positioning with a surface coordinate system (GPS), but not without significant work. Additional effort is needed to automate the point cloud registrations.

Although this project spent time testing and selecting wireless communication radios, the chosen radios were not tested in more than a few real-world tunnel environments. It is therefore strongly recom-

mended that more wireless communication tests be conducted in additional tunnels with various soil types, sizes, shapes, and curvatures.

11. CONCLUSION

The *Counter Tunnel* project has focused on developing UGV solutions to explore, localize, traverse, characterize, and map tunnel-like environments. Work was performed jointly by AFRL (*CTER* snake platform and Borehole Deployment/Retrieval Apparatus) and SSC Pacific (sensor processing, tunnel characterization, wireless communications, localization, and autonomy), with test and demonstration events at both the AFRL Tyndall Mock Test Tunnel and the San Diego border region.

Despite the challenges of integration on a new prototype UGV platform (*CTER*) and the difficult task of localization and mapping in a GPS-denied tunnel environment, the *Counter Tunnel* project individually met all but one of the demanding requirements (the CTER was not tested for water tightness through 20-centimeter standing water). The project successfully demonstrated deployment into and retrieval from a tunnel environment through a 20-centimeter-diameter borehole, climbing 30-centimeter vertical steps, crossing 30-centimeter gaps, transiting over 800 meters round trip, traversing two horizontal 45-degree turns, operating over varied and rough terrain, autonomously exploring, localizing, and mapping a tunnel, generating a 3D model of the tunnel, and locating egress points within 1 meter of accuracy. This project has advanced the state of the art in the areas of platforms, sensors, communications, payloads, GPS-denied navigation, 3D perception, and mapping in the realm of counter-tunnel systems.

REFERENCES

1. Laird, R., Bruch, M., West, M., Ciccimaro, D., and Everett, H. R. 2000. "Issues in Vehicle Teleoperation for Tunnel and Sewer Reconnaissance." Report ADA422071. Space and Naval Warfare Systems Command, San Diego, CA. Available at Defense Technical Information Center. Accessed 23 March 2015.

2. Thrun, S., Ferguson, D., Ha¨hnel, D., Montemerlo, M., Triebel, R., and Burgard, W. 2003. "A System for Volumetric Robotic Mapping of Abandoned Mines." *Proceedings of the IEEE International Conference on Robotics & Automation (ICRA) Volume 3* (pp. 4270–4275). 14–19 September, Taipei, Tawan.

3. Thrun, S., Thayer, S., Whittaker, W., Baker, C., Burgard, W., Ferguson, D., Hähnel, D., Montemerlo, M., Morris, A., Omohundro, Z., Reverte, C., and Whittaker, W. 2004. "Autonomous Exploration and Mapping of Abandoned Mines," *IEEE Robotics and Automation Magazine*, vol. 11, no. 4, p. 79–91.

4. Ferguson, D., Morris, A., Hähnel, D., Baker, C., Omohundro, Z., Reverte, C., Thayer, C., Whittaker, W., Whittaker, W., Burgard, W. and Thrun, S. 2003. "An Autonomous Robotic System for Mapping Abandoned Mines." S. Thrun, L. Saul, and B. Schölkopf, Eds. *Proceedings of Conference on Neural Information Processing Systems (NIPS)*, Cambridge, MA. MIT Press.

5. Nuchter, A., Surmann, H., Lingemann, K., Hertzberg, J., and Thrun, S. 2004. "6D SLAM with an Application in Autonomous Mine Mapping." *Proceedings of the IEEE International Conference on Robotics and Automation* Volume 2 (pp. 1998–2003). 26 May–1 May, New Orleans, LA.

6. Shen, S., Michael, N., and Kumar, V. 2012. "Autonomous Indoor 3D Exploration with a Micro-Aerial Vehicle*." IEEE International Conference on Robotics and Automation* (pp. 9–15). 14–18 May, Saint Paul, MN.

7. Briod, A., Kornatowski, P. M., Klaptocz, A., Garnier, A. , M. Pagnamenta, J. –C. Zufferey, and Floreano, D. 2013. "Contact-based Navigation for an Autonomous Flying Robot." *International Conference on Intelligent Robots and Systems (IROS)* (pp. 3987–3992). 3–7 November, Tokyo, Japan.

8. Brockers, R., Bouffard, P., Ma, J., Matthies, L., and Tomlin, C. 2011. Autonomous Landing an Ingress of Micro-Air-Vehicles in Urban Environments based on Moncular Vision." *Proceedings of SPIE 8031* (pp. 803111–803111–12). 25–29 April, Orlando, FL.

9. Olson, E. 2011. "AprilTag: A Robust and Flexible Visual Fiducial System." *Proceedings of the IEEE International Conference on Robotics and Automation (ICRA)* (pp. 3400–3407). 9–13 May, Shanghai, China.

10. Zhang, Z. 2000. "A Flexible New Technique for Camera Calibration." *IEEE Transactions on Pattern Analysis and Machine Intelligence*, vol. 22, pp. 1330–1334.

11. Okorn, B. 2011. "Smuggling Tunnel Mapping Using Slide Image Registration." Master's thesis, Vanderbilt University.

12. Bradley, D. M., Silver, D., and Thayer, S. 2004. "A Regional Point Descriptor for Global Topological Localization in Flooded Subterranean Environments." *Proceedings of the IEEE Conference on Robotics, Automation and Mechatronics (RAM) Volume 1* (pp. 440–445). 1–3 December, Singapore.

13. Snavely, N., Seitz, S. M., and Szeliski, R. 2008. “Modeling the World from Internet Photo Collections.” *International Journal of Computer Vision*, vol. 80, no. 2, pp. 189–210. Available at http://phototour.cs.washington.edu/. Accessed 23 March 2015.

14. Ahuja, G., Fellars, D., Kogut, G., Rius, E. P., Sights, B., and Everett, H. 2009. “Test Results of Autonomous Behavior for Urban Environment Exploration,” *Proceedings of SPIE Unmanned Systems Technology XI, Volume 7332*. 14–17 April, Orlando, FL.

15. Powell, D., Gilbreath, G., and Bruch, M. 2006. “Multi-robot Operator Control Unit.” *Proceedings of SPIE 6230, Unmanned Systems Technology VIII*. Volume 62301N. 18–20 April, Orlando, FL.

16. Pezeshkian, N., Nguyen, H., and Burmeister, A. 2007. “Unmanned Ground Vehicle Radio Relay Deployment System for Non-line-of-sight Operations.” *Proceedings of the 13th IASTED International Conference on Robotics and Applications* (pp. 501–506). 29–31 August, Wuerzburg, Germany.

REPORT DOCUMENTATION PAGE

Form Approved
OMB No. 0704-01-0188

PLEASE DO NOT RETURN YOUR FORM TO THE ABOVE ADDRESS.

1. REPORT DATE *(DD-MM-YYYY)*	2. REPORT TYPE	3. DATES COVERED *(From - To)*
March 2015	Final	

4. TITLE AND SUBTITLE

Counter Tunnel Project Final Report

5a. CONTRACT NUMBER

5b. GRANT NUMBER

5c. PROGRAM ELEMENT NUMBER

6. AUTHORS

Jacoby Larson
David Hooper
Jim Edwards
Tracy Heath Pastore
Ryan Halterman
Brian Okorn
Brian Skibba
AFRL

5d. PROJECT NUMBER

5e. TASK NUMBER

5f. WORK UNIT NUMBER

7. PERFORMING ORGANIZATION NAME(S) AND ADDRESS(ES)

Air Force Research Laboratory
Airbase Technologies Division
139 Barnes Drive, Suite 2
Tyndall AFB, FL 32403-5323

Space and Naval Warfare Systems Center Pacific
53560 Hull Street
San Diego, CA 92152-5001

8. PERFORMING ORGANIZATION REPORT NUMBER

TR 2071

9. SPONSORING/MONITORING AGENCY NAME(S) AND ADDRESS(ES)

Office of the Under Secretary of Defense for Acquisition, Technology and Logistics
Joint Ground Robotics Enterprise (JGRE) Program
3010 Defense Pentagon
Washington, DC 20301-3010

10. SPONSOR/MONITOR'S ACRONYM(S)

11. SPONSOR/MONITOR'S REPORT NUMBER(S)

12. DISTRIBUTION/AVAILABILITY STATEMENT

Approved for public release.

13. SUPPLEMENTARY NOTES

14. ABSTRACT

The prototype counter-tunnel system developed under this effort is composed of a robotic mobility platform, perception sensor payload, onboard autonomy capability, command and control operator unit, and deployment apparatus. The overall design was driven by the requirement to deploy the system into a tunnel through a 20-centimeter-diameter borehole. This requirement posed many design and packaging challenges for the perception payload and mobility platform in order to fit through the narrow borehole opening and still be able to perform the mission in a GPS-denied environment.

The *Counter Tunnel* project presented a unique prototype UGV mobility platform capable of insertion and retrieval through the 20-centimeter-diameter borehole, climbing 30-centimeter vertical steps, and crossing 30-centimeter gaps. This project also demonstrated a perception system capable of performing obstacle detection, 3D mapping, and GPS-denied localization with an error of less than 0.1% after traveling autonomously for 900 meters through a tunnel-like environment. This project has increased the technology readiness level of various components of the counter-tunnel systems (platforms, sensors, communications, and payloads) and has advanced the work in GPS-denied navigation, 3D perception, and mapping. The prototype evaluations and expertise gained from this work will be key to providing robust and deployable systems to explore tunnels, caves, mines, and similar environments.

15. SUBJECT TERMS

borehole deployment apparatus
counter tunnel exploration robot
system testing and demonstration
localization and mapping
robot autonomy
multi-robot operator control unit
robotic platforms

16. SECURITY CLASSIFICATION OF:			17. LIMITATION OF ABSTRACT	18. NUMBER OF PAGES	19a. NAME OF RESPONSIBLE PERSON
a. REPORT	b. ABSTRACT	c. THIS PAGE			Jacoby Larson
U	U	U	U	63	19B. TELEPHONE NUMBER *(Include area code)* (619) 553-9775

INITIAL DISTRIBUTION

84300	Library	(2)
85300	Archive/Stock	(1)
71710	J. Larson	(1)
71710	T. H. Pastore	(1)
71710	R. Halterman	(1)
71710	B. Okorn	(1)
71720	D. Hooper	(1)
71720	J. Edwards	(1)

Air Force Research Laboratory
Airbase Technologies Division
Attn: Brian Skibba
139 Barnes Drive, Suite 2
Tyndall AFB, FL 32403-5323 (1)

Defense Technical Information Center
Fort Belvoir, VA 22060–6218 (1)

Approved for public release.

SSC Pacific
San Diego, CA 92152-5001